



**NTNU – Trondheim**  
Norwegian University of  
Science and Technology

# Modelling and Test Setup for Sandwich Radomes

**Fredrik Lien**

Electronics System Design and Innovation

Submission date: June 2014

Supervisor: Egil Eide, IET

Co-supervisor: Irene Jensen, Sintef

Norwegian University of Science and Technology  
Department of Electronics and Telecommunications



---

# Problem Description

A large part of the radome market is large dome shaped structures composed of composite panels shaped as pentagons or hexagons. The panels are typically made in a so-called A-sandwich type having a thicker foam core surrounded by thinner layers of composite materials. This makes the panels mechanically strong so that they can be assembled into a self-supporting structure. The joints between the panels consists of a reinforced composite layer, which is mounted with bolts. Radomes are used for protection of various types of antennas, both radar and communications applications, operating in different frequency bands. Radome design must be optimized for each application so that the radio frequency signal is affected minimally. The joints are often included in a solution that will compensate for the loss and unwanted extra proliferation of radio frequency signals. For calculation of the reflection, transmission and losses through the sandwich the structures can be modeled as a series of transmission lines, where thickness, relative permittivity and loss coefficient is included, and where the response is determined using ABCD parameters. By optimizing one or several thicknesses, the radio frequency response can be tuned or optimized for the lowest possible loss for a given frequency band. For an accurate and reliable result it is very important to have accurate values for the material's relative permittivity and loss coefficient. Various types of resonators are used to measure the material's electrical properties. The task will consist of the following:

1. Develop program code in Matlab for up to 10 layers in a sandwich radome to calculate transmission and reflection as a function of frequency and angle. Each layer is a transmission line described with an ABCD matrix, which is further combined to calculate the total response.
2. Develop a program code to optimize for minimum loss of one or more frequency bands by varying one or more thicknesses of the sandwich structure. Develop an optimization method to obtain the best possible match with a measured response by varying the relative permittivity and loss coefficient for a 3-layer sandwich structure.
3. Develop a test setup in a waveguide, where a sample of the sandwich panel is inserted into the waveguide and two-port S-parameters are measured with a network analyzer. Develop a TRL (Thru - Reflect - Line) calibration kit to calibrate out the transitions between the coax probe and the waveguide.
4. Carry out measurements with the waveguide setup and compare simulated results with measurements. Run the optimization routine developed in section 2, alter the relative permittivity and loss coefficient in layers to achieve the best match.

Assignment given: 16. January 2014  
Supervisor: Egil Eide, IET  
Co-Supervisor: Irene Jensen, SINTEF

---

# Summary

Sandwich radomes are structures providing communication- and radar antennas with protection from the environment. The sandwich materials are designed to affect the electromagnetic radiation as little as possible with respect to transmission- and reflection loss, boresight error, boresight error slope, increased sidelobe levels and depolarization. In order to match the frequency response of the radome material to the specifications, simulation and optimization of the thickness and dielectric properties of the individual sandwich layers is done.

To simulate the transmission- and reflection coefficients for sandwich materials a Matlab script has been developed. The script calculate the response for up to 10 different layers for incidence angles and frequencies defined by the user. Verification of the results has been done by comparing the simulated data to results in Kozakoff (2010) and show that the script works correctly.

Waveguide measurement and calibration components have been designed and manufactured in order to measure samples of dielectric materials and samples of complete radome sandwich materials. The results have been compared to results from simulations done in CST Microwave Studio and show a good match for complete sandwich materials and thicker dielectrics. However the measurement results for thin material samples show more deviation compared to the simulation results. The deviation seems to be dependent on the thickness of the sample.

Two optimization routines have been developed in Matlab. The first compare the measured results from measurements to the simulated results from Matlab. Least square optimization is used to adjust the dielectric properties (relative permittivity and dielectric loss tangent) used by the simulation script in order to match the simulation values to the measured values. The results show good match of the optimized relative permittivity for a 22 mm thick sample of Teflon with the optimized value deviating 1.3% from the specified permittivity value. With decreasing thickness of the test samples the deviation increased to approximately 3-12%. The optimized loss tangent values however show very large deviation from the specified values and should be treated as invalid. The main reasons are believed to be the low loss of the materials combined with the thickness relative to the measurement wavelength.

The second optimization routine adjust the thickness of the individual layers to achieve minimum loss for one- or more predefined frequency bands. The results show that the optimization work as intended. To investigate the effect of production errors/production tolerances the core thickness of an A-sandwich has been adjusted with  $\pm 10\%$  from the optimized thickness. The result show that the thickness deviation has a bigger impact on high frequencies.

---

# Sammendrag

Sandwich radomer er strukturer som beskytter kommunikasjons- og radarantenner mot omgivelsene. Sandwich-materialene er designet til å påvirke den elektromagnetiske strålingen så lite som mulig med hensyn på transmisjons- og refleksjonstap, "boresight error", "boresight error slope", økte sidelobe nivåer og depolarisering. For å matche radomens frekvensrespons til spesifikasjonene simuleres og optimaliseres tykkelsen og de dielektriske egenskapene til de enkelte sandwich lagene.

For å simulere transmisjons- og refleksjonskoeffisientene for sandwich-materialer har et Matlab skript blitt utviklet. Skriptet beregner responsen for opp til 10 forskjellige lag for brukerdefinerte innfallsvinkler og frekvenser. Verifisering av resultatene har blitt gjort ved å sammenligne simulerte data med resultater fra Kozakoff (2010) og viser at skriptet fungerer korrekt.

Bølgeleder måle- og kalibreringskomponenter har blitt designet og produsert for å måle prøver av radom sandwich-materialer. Resultatene er sammenlignet med resultater fra simuleringer i CST Microwave Studio og resultatene samsvarer godt for tykkere materialer. Måleresultatene for tynne materialprøver avslører et større avvik i forhold til simuleringsresultatene. Avviket ser ut til å være avhengig av materialtykkelsen.

To optimaliseringsrutiner har også blitt utviklet i Matlab. Den første sammenligner målte resultater fra bølgelederoppsettet med de simulerte resultatene fra Matlab. "Least square" optimalisering brukes til å justere de dielektriske egenskapene (relativ permittivitet og dielektrisk tap) i simuleringsprogrammet for å tilpasse simulerings verdiene til de målte verdiene. Resultatene viser en god match for en 22 mm tykk prøve av teflon der den optimaliserte permittiviteten avviker 1,3% fra angitt permittivitet. De optimaliserte permittivitetene for tynnere materialer har større avvik og ligger i området 3-12%. De optimaliserte tapsverdiene viser svært store avvik fra de angitte verdiene og bør anses som ugyldige. Hovedgrunnen er antatt å være det lave tapet i materialene kombinert med tykkelsen i forhold til bølgelengdene i målingene.

Den andre optimaliseringsrutinen justerer tykkelsen på de enkelte lagene for å oppnå minimum tap for en- eller flere forhåndsdefinerte frekvensbånd. Resultatene viser at optimaliseringen fungerer som forventet. For å undersøke effekten av produksjonsfeil/produksjons toleranser har tykkelsen på kjernen for en A-sandwich blitt justert med  $\pm 10\%$  i forhold til den optimaliserte tykkelsen. Resultatet viser at avvik i tykkelsen har en større innvirkning på høye frekvenser enn på lave.

---

# Preface

This report is the final thesis in the master study in electronic engineering at the Department of Electronics and Telecommunication, Faculty of Information and Technology, at the Norwegian University of Science and Technology (NTNU). The report has been written in the period January 2014 - June 2014 at NTNU.

The work has combined programming in Matlab, mechanical and electrical design and laboratory measurements. The diversity of the work has been motivating and allowed me to gain knowledge on a range of areas such as programming techniques, optimization and curve fitting, waveguide design and measurement techniques.

I would like to thank my supervisors, Egil Eide (NTNU) and Irene Jensen (SINTEF), for good help during my work. I would also like to thank Tore Landsem and Tore Berg at the Department of Electronics and Telecommunications mechanical workshop for the help with producing the test- and calibration components used in the measurements.

Fredrik Lien

# Table of Contents

<b>Problem Description</b>	<b>i</b>
<b>Summary</b>	<b>ii</b>
<b>Sammendrag</b>	<b>iii</b>
<b>Preface</b>	<b>iv</b>
<b>Table of Contents</b>	<b>vi</b>
<b>List of Tables</b>	<b>vii</b>
<b>List of Figures</b>	<b>xi</b>
<b>1 Introduction</b>	<b>1</b>
<b>2 Literature Review</b>	<b>3</b>
2.1 Measurement Technics . . . . .	3
2.2 Multi-layer sandwich characterization . . . . .	3
<b>3 Basic Theory</b>	<b>7</b>
3.1 S-Parameters . . . . .	7
3.2 ABCD-Parameters . . . . .	8
3.3 Permittivity and Dielectric Loss Tangent . . . . .	10
3.4 Radome Wall Transmission . . . . .	11
3.4.1 Radome Types, Classes and Styles . . . . .	11
3.4.2 Boundary Value Solution . . . . .	12
3.5 Rectangular Waveguides . . . . .	17
3.6 Calibration . . . . .	18

---

<b>4</b>	<b>Design</b>	<b>21</b>
4.1	Matlab . . . . .	21
4.1.1	ABCD-Method . . . . .	21
4.2	Matlab ABCD-Method Waveguide Compensation . . . . .	23
4.2.1	Optimization . . . . .	23
4.3	CST Microwave Studio . . . . .	29
4.4	Waveguide Measurement Setup . . . . .	29
4.4.1	Waveguide Measurement and Calibration Kit Design . . . . .	29
<b>5</b>	<b>Measurements and Results</b>	<b>37</b>
5.1	Waveguide Measurements . . . . .	37
5.1.1	Calibration . . . . .	37
5.1.2	Radome Sandwich Sample . . . . .	37
5.1.3	Sample Gap . . . . .	42
5.2	Optimization Results . . . . .	42
5.2.1	Measured Response versus Simulated Response . . . . .	42
5.2.2	Frequency Band Transmission Optimization . . . . .	48
<b>6</b>	<b>Analysis</b>	<b>51</b>
6.1	Matlab ABCD-script . . . . .	51
6.2	Waveguide TRL and Measurement Components . . . . .	51
6.3	Matlab versus Measurement Results . . . . .	52
6.4	Matlab Script for Frequency Band Optimization . . . . .	54
<b>7</b>	<b>Conclusion</b>	<b>57</b>
7.1	Matlab Simulations . . . . .	57
7.2	Waveguide Measurement and Calibration Components . . . . .	57
7.3	Matlab Optimization . . . . .	57
<b>8</b>	<b>Future Work</b>	<b>59</b>
	<b>Bibliography</b>	<b>61</b>
	<b>Appendix</b>	<b>63</b>



# List of Tables

2.1	A general comparison of the microwave dielectric measurement systems (Venkatesh and Raghavan, 2005). . . . .	4
3.1	Conversion between S-parameters and ABCD-parameters. . . . .	9
3.2	Frequency band vs. rectangular cross section dimensions (a x b). . . . .	18
4.1	Matlab ABCD-script parameters. . . . .	21
4.2	<i>lsqnonlin</i> input arguments. . . . .	26
4.3	<i>fminsearchbnd</i> input arguments. . . . .	27
4.4	<i>Optimization.m</i> input arguments. . . . .	27
4.5	<i>Wall_Transmission_Optimization.m</i> input parameters and data. . . . .	28
4.6	<i>Optimization_Frequency_Band.m</i> input parameters and data. . . . .	28
4.7	<i>Wall_Transmission_Optimization_Frequency_Band.m</i> input parameters and data. . . . .	28
4.8	Coax-to-Waveguide design parameters. . . . .	30
5.1	Material properties for the measured sandwich sample. . . . .	38
5.2	Optimization results for measured response values versus simulated response. Values marked with * indicate that the upper/lower bound of the optimization was reached. . . . .	43
5.3	Optimization results for transmission at given frequency band(s). . . . .	48
5.4	Frequency band deviation with $\pm 10\%$ thickness deviation. . . . .	49
6.1	Optimization results for measured response values versus simulated response. Values marked with * indicate that the upper/lower bound of the optimization was reached. . . . .	54
6.2	Permittivity and loss tangent Teflon (PTFE). The loss tangents were not optimized as their values proved to have little or no effect on the optimization results. . . . .	54

---

---

# List of Figures

3.1	Two-port network (Pozar, 2011). . . . .	8
3.2	Transmission line section of length $\Delta x = d/n$ (Peres et al., 2004). . . . .	9
3.3	Reflected and transmitted waves at a discontinuity interface (Collin, 1991). . . . .	13
3.4	Terminal planes for a discontinuity (Collin, 1991). . . . .	14
3.5	Cascade connection of $n$ sections (Collin, 1991). . . . .	15
3.6	Boundary value solution of the N-layer dielectric wall radome (Kozakoff, 2010). . . . .	16
3.7	Waveguide dimensions. . . . .	17
3.8	DUT with error boxes (Pozar, 2011). . . . .	19
4.1	Flowchart for the Matlab ABCD script. . . . .	22
4.2	Half-wave wall transmission, perpendicular polarization ( $t = 0.8255cm$ , $\epsilon_r = 4$ , $\tan\delta = 0.015$ ). . . . .	23
4.3	A-sandwich transmission, perpendicular polarization (skins: $t = 0.0762cm$ , $\epsilon_r = 3.23$ , $\tan\delta = 0.016$ , core: $t = 1.016cm$ , $\epsilon_r = 1.1$ , $\tan\delta = 0.001$ ). . . . .	24
4.4	C-sandwich transmission, perpendicular polarization (skins: $t = 0.0762cm$ , $\epsilon_r = 3.23$ , $\tan\delta = 0.016$ , cores: $t = 0.5842cm$ , $\epsilon_r = 1.1$ , $\tan\delta = 0.001$ ). . . . .	24
4.5	Seven-layer wall transmission, perpendicular polarization (skins: $t = 0.0762cm$ , $\epsilon_r = 3.23$ , $\tan\delta = 0.016$ , cores: $t = 0.3302cm$ , $\epsilon_r = 1.1$ , $\tan\delta = 0.001$ ). . . . .	25
4.6	CST Microwave Studio simulation of WR284 waveguide with sandwich insert. . . . .	29
4.7	Comparison between ABCD-simulation in Matlab and simulation in CST Microwave Studio. (layer 1: $t = 3.0cm$ , $\epsilon_r = 1.08$ , $\tan\delta = 0.001$ , layer 2: $t = 4.0cm$ , $\epsilon_r = 3.8$ , $\tan\delta = 0.001$ ). . . . .	30
4.8	SMA to waveguide adapter design parameters (Microwaves101, 2013). . . . .	31
4.9	S11 for SMA to waveguide adapter. . . . .	32
4.10	S21 for SMA to waveguide adapter. . . . .	32
4.11	SMA to waveguide adapter. . . . .	33
4.12	Reflection component for TRL calibration kit. . . . .	34
4.13	Line component for TRL calibration kit. . . . .	35

---

4.14	Sample holder for waveguide measurement setup. . . . .	36
4.15	Through, reflect, line calibration on ANA. . . . .	36
5.1	Uncalibrated S11 values versus calibrated S11 values, empty waveguide. .	37
5.2	Uncalibrated S21 values versus calibrated S21 values, empty waveguide. .	38
5.3	Radome sandwich sample cut to inner waveguide dimensions. . . . .	39
5.4	Radome sandwich sample inserted in sample holder. . . . .	39
5.5	Waveguide measurement test setup and ANA. . . . .	40
5.6	Measured S11 values from complete radome sandwich and the individual layers. . . . .	40
5.7	Measured S21 values from complete radome sandwich and the individual layers. . . . .	41
5.8	Comparison between the S11 values for a radome sandwich element with different gaps between sample and waveguide. . . . .	42
5.9	Comparison between the measured and simulated reflection coefficients before and after optimization of the relative permittivity and loss tangent for the radome sandwich sample . . . . .	43
5.10	Comparison between the measured and simulated transmission coefficients before and after optimization of the relative permittivity and loss tangent for the radome sandwich sample. . . . .	44
5.11	Comparison between the measured and simulated reflection coefficients before and after optimization of the relative permittivity and loss tangent for the core layer of the radome sandwich sample. . . . .	44
5.12	Comparison between the measured and simulated transmission coefficients before and after optimization of the relative permittivity and loss tangent for the core layer of the radome sandwich sample. . . . .	45
5.13	Comparison between the measured and simulated reflection coefficients before and after optimization of the relative permittivity and loss tangent for the laminate and gelcoat layer of the radome sandwich sample. . . . .	45
5.14	Comparison between the measured and simulated transmission coefficients before and after optimization of the relative permittivity and loss tangent for the laminate and gelcoat layer of the radome sandwich sample. . . . .	46
5.15	Comparison between the measured and simulated reflection coefficients before and after optimization of the relative permittivity and loss tangent for a sample of FR4 substrate. . . . .	46
5.16	Comparison between the measured and simulated transmission coefficients after optimization of the relative permittivity and loss tangent for a sample of FR4 substrate. . . . .	47
5.17	Transmission loss coefficient for a 1 layer Half-wave wall optimized for 8 – 12GHz (X-band). . . . .	48
5.18	Transmission loss coefficient for a 1 layer Half-wave wall optimized for 14 – 16GHz. . . . .	49
5.19	Transmission loss coefficient for a 3 layer A-sandwich optimized for 7 – 8GHz and 18 – 19GHz. . . . .	50

---

---

5.20	Comparison of the transmission loss for an A-sandwich with optimized thickness of the core, 10% reduced thickness of the core and 10% increased thickness of the core. . . . .	50
6.1	Dependence of the computed permittivity on the thickness error (Olmi et al., 2002). . . . .	52

# Chapter 1

## Introduction

Radomes are structures designed to protect radar and communication antennas against the environment. The main design goal for the radome is to minimize the impact on the electromagnetic radiation and at the same time provide protection by means of a self supporting structure without an inner framework. This is mostly done by using composite sandwich materials. The sandwich usually consist of a core material made of a foam or honeycomb material with low dielectric value between thin laminates with a higher dielectric value.

In order to design the radome sandwich material the thickness and dielectric properties of the layers have to be calculated. For most multi layered materials the laminate on either side of the core is kept fixed and the thickness of the core material is adjusted. Adjustment of the core thickness allows the designers to minimize the transmission loss, the reflection loss and the boresight error for given frequencies.

Sandwich radomes are used on a number of platforms such as aircrafts, ships, land based vehicles and stationary systems. The application of the system define additional design requirements such as aerodynamics, strength, boresight error requirements etc.

The report is structured as follows: Chapter 2 present some of the techniques used today for measuring the properties of dielectric materials and multi-layer sandwich characterization, chapter 3 give a presentation of basic theory for characterization of sandwich materials where the most important formulas are derived, chapter 4 describe the design process of the physical test equipment and the different matlab-scripts together with example results, chapter 5 present the results from the waveguide test setup measurements and the optimization routines, chapter 6 discuss the results from the measurements presented in chapter 5 and in chapter 7 the conclusion and thoughts of future work is presented.

---

# Literature Review

## 2.1 Measurement Technics

For manufacturers of radome-materials and radomes, characterization of the finished sandwich structure in order to determine the actual dielectric properties is important. If the material properties differ largely from the specifications it can lead to a shift in the radome frequency band. As a consequence the desired frequency band can possibly be attenuated with possible increased loss and boresight errors. Baker-Jarvis et al. (2005), ASTM International (2008) and Tereschenko et al. (2011) propose a method for material measurements using coaxial lines or waveguides. A sample of the sandwich material is placed inside the coaxial line or waveguide, an electromagnetic field is introduced and the scattering parameters are measured. The material properties can also be calculated by solving the boundary-value problem in waveguides and coaxial lines. It is assumed for these calculations that only the fundamental mode,  $TE_{10}$  in waveguides and TEM in coaxial lines, is propagating. Another method proposed by Baker-Jarvis et al. (2005) and Tereschenko et al. (2011) is free space measurement. In this method antennas are used to measure the TEM transmission and reflection coefficients. The sample is placed between two antennas and a calibration is done to minimize the scattering effects of objects in the vicinity of the test rig. To obtain the values of the sample a similar method as for coaxial line and waveguide measurements is used.

Other methods are also available for the measurement for lossy materials. Table 2.1 list measurement techniques including frequency band, sample size requirements, temperature control, accuracy, sample preparation, suitable test materials, measured parameter, destructive/non-destructive to test material and if commercial vendors exist.

## 2.2 Multi-layer sandwich characterization

The method to model multi-layer radome structures as transmission lines with different length and electrical properties, used in this thesis, is a well proven technique described



**Table 2.1:** A general comparison of the microwave dielectric measurement systems (Venkatesh and Raghavan, 2005).

	<b>Slotted line reflection system</b>	<b>Guided wave transmission system</b>	<b>Free space transmission system</b>	<b>Filled cavity resonance system</b>	<b>Partially filled cavity resonance system</b>	<b>Probe reflection system</b>
Frequency	broad band	banded	banded	single	single	broad band
Sample size	moderate	moderate	large	large	very small	small
Temperature monitoring/control	difficult	difficult	very easy	very easy	very easy	easy
Accuracy for:						
Low-loss material	very low	moderate	moderate	very high	high	low
High-loss material	low	moderate	moderate	does not work	low	high
Sample preparation	easy	difficult	easy	very difficult	very difficult	easy
Most suitable test material	solids, semisolids	solids	large flat sheets	solids, semisolids, liquids	solids	solids, semisolids, liquids
Measured parameter	permittivity	permittivity and permeability	permittivity and permeability	permittivity or permeability	permittivity or permeability	permittivity
To test material	destructive	destructive	non-destructive	destructive	destructive	non-destructive
Commercial vendors	no	yes	yes	no	no	yes

in several papers. Among others, Wegner and Lobue (1964), Collin (1991) and Kedar and Revankar (2006) all describe this method. Collin (1991) shows that if the transmission

---

lines are characterized using ABCD parameters, the calculation of the response through the structure can be done in a convenient manner by simply multiplying the ABCD-matrices for the different layers. Virone et al. (2007) propose a method of measuring a sample of the sandwich completely filling the cross section of a waveguide. The measurement data are then compared to a simulation of the same material using ABCD-parameters. Finally a least-square fitting is done to adjust the ABCD-parameter response for best match between the measured and simulated response by changing the dielectric properties of the individual layers, assuming the thickness is fixed.

---

---

# Basic Theory

## 3.1 S-Parameters

The scattering matrix is a mathematical tool that quantifies how RF-energy propagates through a n-port network. S-parameters allows to accurately describe properties of complicated networks as "black-boxes". For a RF-signal input on one port, a bit of the signal is reflected and return out of the same port, some of it scatters and exits other ports, sometimes amplified, and some of the signal is dissipated, for instance as heat or radiomagnetic radiation. The S-matrix for a N-port have  $N^2$  coefficients or S-parameters where every coefficient describe a possible input-output path. S-parameters are complex values, hence they include both a magnitude and an angle. This is because both the magnitude and angle of a signal is potentially changed by the network. However, the magnitude is usually the value of interest. Basically S-parameters describe the RF-voltage out versus RF-voltage in. The S-parameter have subscripts "ij", where "j" is the port excited and "i" is the output port. Thus S11 refers to the ratio of the signal reflected on port one for a signal incident on port one. The input and output reflection coefficients of N-port networks, S11 and S22 for a 2-port, can be visualized on the Smith chart. As mentioned above, S-parameters describe the response of a N-port network to RF-voltage signals at each port. In a two-port network, the input voltage at each port is denoted by  $V_1$  while the voltage leaving the port is denoted by  $V_2$ . With the assumption that the ports is terminated in the impedance  $Z_0$  the four parameters of the 2-port are defined as (Pozar, 2011):

$$S_{11} = \frac{V_1^-}{V_1^+}, S_{12} = \frac{V_1^-}{V_2^+}, S_{21} = \frac{V_2^-}{V_1^+}, S_{22} = \frac{V_2^-}{V_2^+} \quad (3.1)$$

The matrix representation of the S-parameters is presented in equation 3.2

$$\begin{bmatrix} V_1^- \\ V_2^- \end{bmatrix} = \begin{bmatrix} S_{11} & S_{12} \\ S_{21} & S_{22} \end{bmatrix} \begin{bmatrix} V_1^+ \\ V_2^+ \end{bmatrix} \quad (3.2)$$

---

## 3.2 ABCD-Parameters

The S-parameter representation is in general a good way to describe microwave networks with N-ports. However most real-world networks consist of several cascaded two-port networks. Using S-parameters for cascaded networks is possible but the math will get very complicated with a high number of microwave networks. A more convenient method to analyze a cascaded two-port network is to use ABCD-parameters. ABCD-parameters can be used to characterize the behavior of linear networks and in contrast to S-parameters provide an efficient way to compute the response of cascaded two-port networks. The ABCD-parameter method define a  $2 \times 2$  ABCD matrix for the individual two-port networks. The cascade of two-port networks is found by multiplying the individual ABCD matrices.

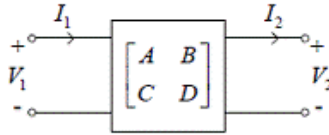


**Figure 3.1:** Two-port network (Pozar, 2011).

The ABCD matrix for the two-port network shown in figure 3.1 is defined by looking at the total voltages and currents (Pozar, 2011):

$$\begin{bmatrix} V_1 \\ I_1 \end{bmatrix} = \begin{bmatrix} A & B \\ C & D \end{bmatrix} \begin{bmatrix} V_2 \\ I_2 \end{bmatrix} \quad (3.3)$$

To make the definition of the ABCD matrix correct for cascaded networks the sign of  $I_2$  is defined such that the current flows out of port 2. In a cascaded network the current  $I_2$  will be the current that continue into the next two-port network. Consequently the left side of equation 3.3 will be the voltage and current of port 1 while the right hand side of equation 3.3 will be the voltage and current of port 2. With two two-port networks in cascade this can be written as

$$\begin{bmatrix} V_1 \\ I_1 \end{bmatrix} = \begin{bmatrix} A & B \\ C & D \end{bmatrix} \begin{bmatrix} V_2 \\ I_2 \end{bmatrix} \quad (3.4)$$

$$\begin{bmatrix} V_2 \\ I_2 \end{bmatrix} = \begin{bmatrix} A & B \\ C & D \end{bmatrix} \begin{bmatrix} V_3 \\ I_3 \end{bmatrix} \quad (3.5)$$

By substituting 3.5 into 3.4 the result is

$$\begin{bmatrix} V_1 \\ I_1 \end{bmatrix} = \begin{bmatrix} A_1 & B_1 \\ C_1 & D_1 \end{bmatrix} \begin{bmatrix} A_2 & B_2 \\ C_2 & D_2 \end{bmatrix} \begin{bmatrix} V_2 \\ I_2 \end{bmatrix} \quad (3.6)$$

From equation 3.6 it is evident that the cascaded ABCD matrix of the two two-port networks is simply the product of the ABCD matrices of network 1 and 2 respectively. In order for this to be correct the multiplication of the networks has to be done in the same order as the connection of the networks (Pozar, 2011).

Another benefit from using ABCD matrix representation is that ABCD matrices of simple two-port networks can be used to build more complicated networks consisting of cascades of the simpler two-port networks.

The ABCD matrix is also easily converted to other two-port networks. The conversion from ABCD-parameters to S-parameters is given in table 3.1 (Pozar, 2011).

**Table 3.1:** Conversion between S-parameters and ABCD-parameters.

<b>ABCD</b>	
$S_{11}$	$\frac{A+B/Z_0-CZ_0-D}{A+B/Z_0+CZ_0+D}$
$S_{12}$	$\frac{2(AD-BC)}{A+B/Z_0+CZ_0+D}$
$S_{21}$	$\frac{2}{A+B/Z_0+CZ_0+D}$
$S_{22}$	$\frac{-A+B/Z_0-CZ_0+D}{A+B/Z_0+CZ_0+D}$

For this thesis the ABCD parameters for transmission lines will be applied. To define the ABCD matrix for a transmission line take a line with length  $d$ , resistance  $r$ , inductance  $l$ , conductance  $g$  and capacitance  $c$ . Dividing the line into  $n$  sections of equal length  $\Delta x$ , each section can be represented by the equivalent circuit shown in figure 3.2 (Peres et al., 2004).

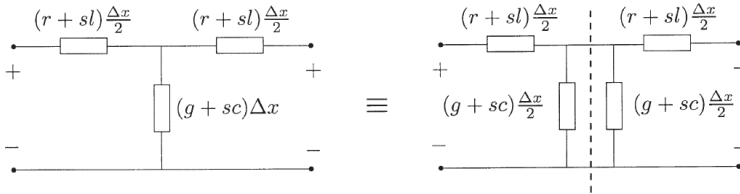


**Figure 3.2:** Transmission line section of length  $\Delta x = d/n$  (Peres et al., 2004).

Splitting the network in figure 3.2 in two the short-circuit and the open-circuit impedances of the left-side section of the splitted network are given by (Peres et al., 2004)

$$z_{sc} = (r + sl) \frac{\Delta x}{2} \quad (3.7)$$

$$z_{oc} = (r + sl) \frac{\Delta x}{2} + \frac{1}{(g + sc) \frac{\Delta x}{2}} \quad (3.8)$$

From equations 3.7 and 3.8 the characteristic impedance  $z_{0k}$  and the propagation constant  $\theta_k$  of the  $k$ th section of length  $\Delta x$  can be obtained (Peres et al., 2004)

---


$$z_{0k} = Z_0 \left( 1 + \left( \gamma \frac{\Delta x}{2} \right)^2 \right)^{1/2} \quad (3.9)$$

$$\tanh \frac{\theta_k}{2} = \gamma \frac{\Delta x}{2} \left( 1 + \left( \gamma \frac{\Delta x}{2} \right)^2 \right)^{-1/2} \quad (3.10)$$

where

$$Z_0 = \frac{r + sl}{g + sc} \quad (3.11)$$

and

$$\gamma = \sqrt{(r + sl)(g + sc)} \quad (3.12)$$

As  $\Delta x$  approaches zero, equation 3.9 shows that  $z_{0k}$  approaches  $Z_0$  and equation 3.10 shows that  $\theta_k$  approaches zero. The section number  $n$  approaches infinity at the same time and the product  $n\Delta x$  (the length  $d$  of the line) remains constant (Peres et al., 2004). The two-port network consisting of  $n$  symmetric reciprocal two-port networks with the same characteristic impedance  $Z_0$  and propagation constants  $\theta_1; \theta_2; \dots; \theta_n$  have an equivalent characteristic impedance  $Z_0$  and the propagation constant  $\theta$  is given by (Peres et al., 2004)

$$\theta = \sum_{k=1}^n \theta_k \quad (3.13)$$

The first-order approximation for  $\theta_k$  is  $\gamma\Delta x$ , equation 3.13 give the line propagation constant  $\theta = \gamma d$  (Peres et al., 2004).

Equation 3.11, 3.12 and 3.14 show the ABCD matrix modelled to a two-wire transmission line of length  $d$  (Peres et al., 2004).

$$\begin{bmatrix} V_1 \\ I_1 \end{bmatrix} = \begin{bmatrix} \cosh(\gamma d) & Z_0 \sinh(\gamma d) \\ \frac{1}{Z_0} \sinh(\gamma d) & \cosh(\gamma d) \end{bmatrix} \begin{bmatrix} V_2 \\ I_2 \end{bmatrix} \quad (3.14)$$

### 3.3 Permittivity and Dielectric Loss Tangent

Permittivity and dielectric loss tangent are important parameters to characterize when working with radome design and characterization. The permittivity and loss tangent of the materials used, together with the thickness of the materials, decide the transmission- and reflection coefficients of the radome wall.

Permittivity is basically a measure of the resistance when forming an electric field in a medium. The permittivity of free space is called  $\epsilon_0$  and the value is  $8.85418782 \cdot 10^{-12}$ . Relative permittivity  $\epsilon_r$  is a commonly used measure on the permittivity for a given material relative to the permittivity of free space. To characterize lossy materials the complex permittivity include a real value  $\epsilon'$  and a complex value  $\epsilon''$ :

---


$$\epsilon = \epsilon' - j\epsilon'' \quad (3.15)$$

The dielectric loss tangent is defined as the ratio between the real and complex permittivity value:

$$\tan \delta = \frac{\epsilon''}{\epsilon'} \quad (3.16)$$

## 3.4 Radome Wall Transmission

Most radars and antennas employed outdoors require some sort of protection from the environment (rain, snow, debris, etc). In the early years of microwave sensors plexiglass and plywood were used to construct radomes. As plywood has moisture absorption problems new materials were developed. The MIT Radiation Laboratory developed a three-layer A-sandwich in 1944. The A-sandwich used dense skins and a low-density core material (Kozakoff, 2010). The method of using combinations of materials with different material properties is still used today. Antenna radomes are usually a sandwich construction utilizing the electrical properties of the layers to maximize transmission in the desired frequency band(s). The different radome styles is described in subsection 3.4.1. Antenna-radomes have effects on the radiation pattern which have to be accounted for in the design process. These effects include *Boresight Error* and *Boresight Error Slope, Increased Sidelobe Levels, Depolarization* and *Insertion Loss* (Kozakoff, 2010).

Several methods to investigate the performance of radome-antenna systems have been developed. These methods can be categorized in 1) High-frequency methods; 2) Low-frequency methods and 3) Analytical methods. However, for most real-world radomes, the assumption that the radome structures have smooth surfaces and electrically large radii of curvature is valid (Kedar and Revankar, 2006). For the simulations in this thesis the sandwich materials have been analyzed using the boundary value solution technique which is a high-frequency method. This method is described in subsection 3.4.2.

### 3.4.1 Radome Types, Classes and Styles

MIL-R-7705B (1988) define 6 radome types, 3 radome classes and 5 radome styles;

- *Type I*: Low-frequency radomes used at frequencies at or below 2.0 GHz.
- *Type II*: Directional guidance radomes having specified directional accuracy requirements. These include boresight error (BSE), boresight error slope (BSES), antenna pattern distortion, and antenna sidelobe degradation.
- *Type III*: Narrowband radomes with an operational bandwidth of less than 10%.
- *Type IV*: Multiple-frequency band radomes used at two or more narrow frequency bands.
- *Type V*: Broadband radomes generally providing an operational bandwidth between 0.100 and 0.667 GHz.



- 
- *Type VI:* Very broadband radomes that provide an operational bandwidth greater than 0.667 GHz.
  - *Class I:* Flight vehicles .
  - *Class II:* Surface vehicles.
  - *Class III:* Fixed ground installations.
  - *Style a.* Half-wave wall. The wall thickness of the radome is one-half wavelength at the design incidence angle and frequency.
  - *Style b.* Thin-wall. The wall thickness of the radome is less than one-tenth wavelength at the design incidence angle and frequency.
  - *Style c.* A sandwich. The wall of the radome is constructed of three layers: two skins and a core material. The dielectric constant of the skin materials is higher than the dielectric constant of the core material.
  - *Style d.* Multilayer sandwich. The wall of the radome is constructed of some odd number of layers of skins and cores greater than three.
  - *Style e.* Dielectrically loaded form core sandwich. The wall of the radome is constructed of three layers: two skins and a dielectrically loaded foam core. The core material is dielectrically loaded to match the dielectric constant of the skin materials. Wall thickness is essentially the same as style a.

### 3.4.2 Boundary Value Solution

To characterize the transmission and reflection coefficients for a radome sandwich material it can be modeled as a multilayer dielectric. Before deriving the matrix for transmission through a multilayer dielectric the wave matrix for a single plane-discontinuity interface will be derived.

From figure 3.3, a TEM wave with amplitude  $C_1$  is incident from the left and a wave of amplitude  $B_2$  is incident from the right. In the  $z < 0$  region there will be a wave consisting of both a reflected wave from the left side and a transmitted wave from the right side. This wave will propagate in the negative  $z$  direction. The same is happening for the  $z > 0$  region where a combined wave will propagate in the positive  $z$  direction. The positive and negative propagating waves can be denoted  $B_1$  and  $C_2$  (Collin, 1991):

$$B_1 = R_1 C_1 + T_{21} B_2 \quad (3.17)$$

$$C_2 = R_2 B_2 + T_{12} C_1 \quad (3.18)$$

or

$$B_1 = \left( T_{21} - \frac{R_1 R_2}{T_{12}} \right) B_2 + \frac{R_1}{T_{12}} C_2 \quad (3.19)$$

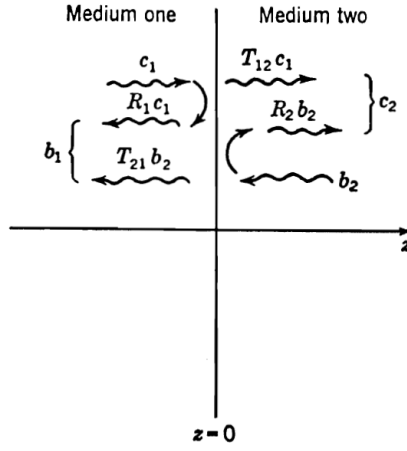


**Figure 3.3:** Reflected and transmitted waves at a discontinuity interface (Collin, 1991).

$$C_1 = \frac{C_2}{T_{12}} - \frac{R_2 B_2}{T_{12}} \quad (3.20)$$

In equations 3.17,3.18,3.19 and 3.20  $R_1$  and  $R_2$  are the reflection coefficients for the interface, and  $T_{12}$  and  $T_{21}$  are the transmission coefficients. In matrix form (Collin, 1991):

$$\begin{bmatrix} C_1 \\ B_1 \end{bmatrix} = \frac{1}{T_{12}} \begin{bmatrix} 1 & -R_2 \\ R_1 & T_{12}T_{21} - R_1R_2 \end{bmatrix} \begin{bmatrix} C_2 \\ B_2 \end{bmatrix} = \begin{bmatrix} A_{11} & A_{12} \\ A_{21} & A_{22} \end{bmatrix} \begin{bmatrix} C_2 \\ B_2 \end{bmatrix} \quad (3.21)$$

The matrix  $[A]$  give the relation between the amplitudes of the forward- and backward-propagating waves on the output side to the waves on the input side. The equivalent transmission and reflection coefficients are given by (Collin, 1991):

$$R_1 = \left. \frac{B_1}{C_1} \right|_{B_2=0} \quad (3.22)$$

$$R_2 = \left. \frac{C_2}{B_2} \right|_{B_2=0} \quad (3.23)$$

$$T_{12} = \left. \frac{C_2}{C_1} \right|_{B_2=0} \quad (3.24)$$

$$T_{21} = \left. \frac{B_1}{B_2} \right|_{B_2=0} \quad (3.25)$$

Together with equation 3.21 these equations define  $A_{ij}$ .

Normalizing the amplitudes  $C_1$ ,  $B_1$ ,  $C_2$  and  $B_2$  the determinant for the matrix  $[A]$  is (Collin, 1991)

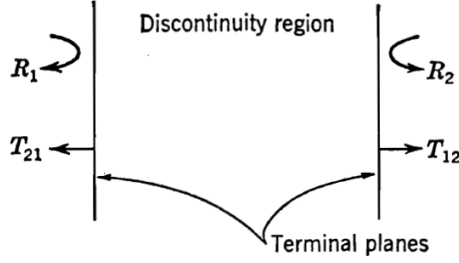


**Figure 3.4:** Terminal planes for a discontinuity (Collin, 1991).

$$A_{11}A_{22} - A_{12}A_{21} = 1 \quad (3.26)$$

For the discontinuity in figure 3.4 the matrix elements  $A_{ij}$  can be written as (Collin, 1991):

$$A_{11} = \frac{1}{T_{12}} \quad (3.27)$$

$$A_{12} = -\frac{R_2}{T_{12}} = \frac{R_1}{T_{12}} \quad (3.28)$$

$$A_{21} = \frac{R_1}{T_{12}} \quad (3.29)$$

$$A_{22} = \frac{T_{12}T_{21} - R_1R_2}{T_{12}} = \frac{1}{T_{12}} \quad (3.30)$$

since  $R_2 = -R_1$ ,  $1 + R_1 = T_{12}$ ,  $1 + R_2 = T_{21}$ . Because of this equation 3.21 can be written as

$$\begin{bmatrix} C_1 \\ B_1 \end{bmatrix} = \frac{1}{T_{12}} \begin{bmatrix} 1 & R_1 \\ R_1 & 1 \end{bmatrix} \begin{bmatrix} C_2 \\ B_2 \end{bmatrix} \quad (3.31)$$

In order to calculate a cascade of  $n$  sections a wavetransmission matrix for a "length of free space" has to be defined. Looking at a forward- and backward-propagating wave,  $C_1e^{-jkz}$  and  $B_1e^{jkz}$  respectively, at  $z = 0$  the amplitudes of the waves are  $C_1$  and  $B_1$ . At  $z = z_1$  the complex amplitude of the waves are  $C_1e^{-jkz_1}$  and  $B_1e^{jkz_1}$ . The amplitude of these two waves are called  $C_2$  and  $B_2$  respectively and (Collin, 1991):

$$C_1 = C_2e^{jkz_1} \quad (3.32)$$

$$B_1 = B_2e^{-jkz_1} \quad (3.33)$$

The electrical length from  $z = 0$  to  $z = z_1$  is  $kz_1$ . Adding the electrical length in equation 3.32 and 3.33:

$$\begin{bmatrix} C_1 \\ B_1 \end{bmatrix} = \begin{bmatrix} e^{jkz_1} & 0 \\ 0 & e^{-jkz_1} \end{bmatrix} \begin{bmatrix} C_2 \\ B_2 \end{bmatrix} \quad (3.34)$$

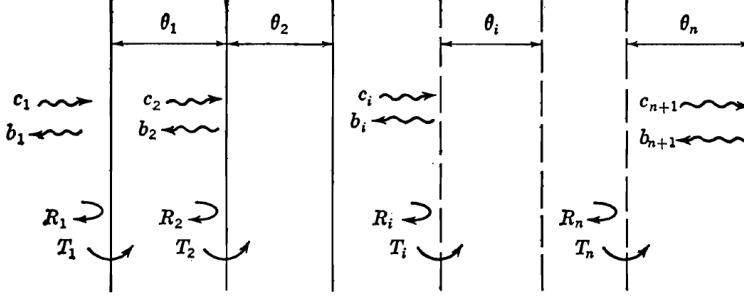


**Figure 3.5:** Cascade connection of  $n$  sections (Collin, 1991).

With  $n$  sections in cascade with  $\epsilon_i$  and  $\tan \delta_i$ , the propagation constant is  $\gamma_i = k_0 \sqrt{\epsilon_{ri} - \sin^2 \theta}$  for the  $i$ th section. If the thickness of the  $i$ th section is  $t_i$  the electrical length become  $\gamma_i t_i$ . Looking at figure 3.5,  $R_i$  and  $T_i$  are the reflection and transmission coefficients respectively when looking into the  $i$ th section.  $R_i$  is the reflection coefficient from section  $i - 1$  and  $T_i$  is the amplitude transmission coefficient from section  $i - 1$  to section  $i$ . Consequently the amplitudes  $C_2, B_2$  are related at the input to section 2 to  $C_1$  and  $B_1$  as (Collin, 1991):

$$\begin{bmatrix} C_1 \\ B_1 \end{bmatrix} = \frac{1}{T_1} \begin{bmatrix} e^{j\gamma_1 t_1} & 0 \\ 0 & e^{-j\gamma_1 t_1} \end{bmatrix} \begin{bmatrix} C_2 \\ B_2 \end{bmatrix} = \frac{1}{T_1} \begin{bmatrix} e^{j\gamma_1 t_1} & R_1 e^{-j\gamma_1 t_1} \\ R_1 e^{-j\gamma_1 t_1} & e^{-j\gamma_1 t_1} \end{bmatrix} \begin{bmatrix} C_2 \\ B_2 \end{bmatrix} \quad (3.35)$$

The output amplitudes  $C_{n+1}, B_{n+1}$  for  $n$  sections in cascade can be related to  $C_1$  and  $B_1$  by taking the matrix product of the  $n$  matrices for each section (Collin, 1991):

$$\begin{bmatrix} C_1 \\ B_1 \end{bmatrix} = \left[ \prod_{i=1}^N \frac{1}{T_i} \begin{bmatrix} e^{j\gamma_i t_i} & R_i e^{-j\gamma_i t_i} \\ R_i e^{-j\gamma_i t_i} & e^{-j\gamma_i t_i} \end{bmatrix} \right] \begin{bmatrix} C_{N+1} \\ B_{N+1} \end{bmatrix} \quad (3.36)$$

The final solution for  $n$  different layers is given by (Kozakoff, 2010):

$$\begin{bmatrix} C_1 \\ B_1 \end{bmatrix} = \left[ \prod_{i=1}^N \frac{1}{T_i T_{N-1}} \begin{bmatrix} e^{j\gamma_i t_i} & R_i e^{-j\gamma_i t_i} \\ R_i e^{-j\gamma_i t_i} & e^{-j\gamma_i t_i} \end{bmatrix} \right] \frac{1}{T_{N+1}} \begin{bmatrix} 1 & R_{N+1} \\ R_{N+1} & 1 \end{bmatrix} \begin{bmatrix} C_{N+1} \\ B_{N+1} \end{bmatrix} \quad (3.37)$$

The Fresnel reflection and transmission coefficients of the  $i$ 'th layer are found from equation 3.38 and 3.39

$$R_i = \frac{Z_i - Z_{i-1}}{Z_i + Z_{i-1}} \quad (3.38)$$

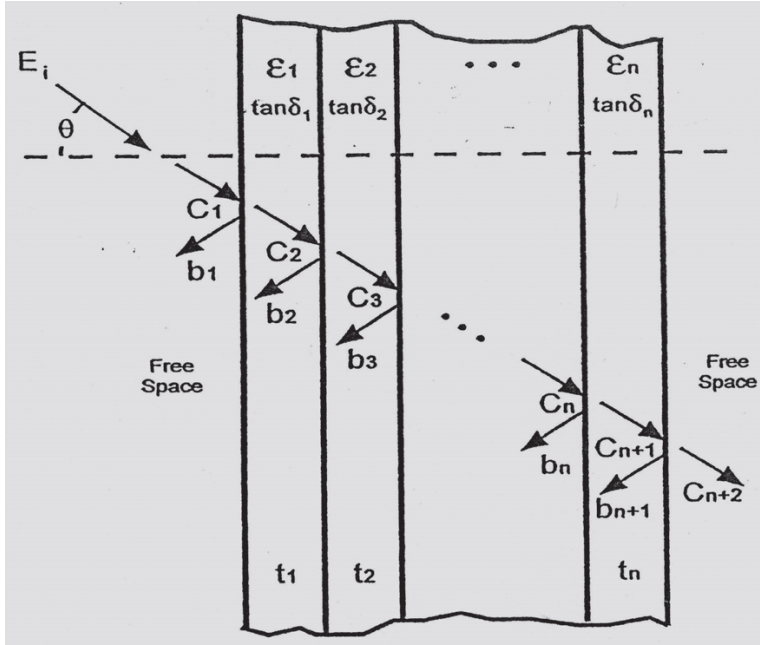


**Figure 3.6:** Boundary value solution of the N-layer dielectric wall radome (Kozakoff, 2010).

$$T_i = \sqrt{1 - R_i^2} \quad (3.39)$$

In order to calculate the Fresnel coefficients the impedance of the individual layers have to be found. The impedances are dependent on the polarization of the incident electromagnetic field. For perpendicular (TE) polarization (Kozakoff, 2010):

$$Z_i = \frac{\cos \theta}{\sqrt{\epsilon_{ri} - \sin^2 \theta}} \quad (3.40)$$

and for parallel (TM) polarization (Kozakoff, 2010):

$$Z_i = \frac{\sqrt{\epsilon_{ri} - \sin^2 \theta}}{\epsilon_{ri} \cos \theta} \quad (3.41)$$

Because of dielectric loss in the layers, a new  $\epsilon_{ri}$  is defined as (Kozakoff, 2010):

$$\epsilon_{ri} = \epsilon'_{ri}(1 - j \tan \delta_i) \quad (3.42)$$

where  $\epsilon'_{ri}$  is the real part of the  $i$ 'th layer and  $\tan \delta_i$  is the loss tangent for the dielectric material.

The final matrix result is found after calculating the matrix product in equation 3.37 (Kozakoff, 2010):

$$\begin{bmatrix} C_1 \\ B_1 \end{bmatrix} = \begin{bmatrix} A_{11} & A_{12} \\ A_{21} & A_{22} \end{bmatrix} \begin{bmatrix} C_{N+2} \\ B_{N+2} \end{bmatrix} \quad (3.43)$$

The reflection voltage coefficient from the sandwich is found by calculating (Kozakoff, 2010):

$$R_w = \frac{B_1}{C_1} \Big|_{(B_{N+2}=0)} = \frac{A_{21}}{A_{11}} \quad (3.44)$$

and the transmission voltage coefficient is found by calculating (Kozakoff, 2010):

$$T_w = \frac{C_{N+2}}{C_1} \Big|_{(B_{N+2}=0)} = \frac{1}{A_{11}} \quad (3.45)$$

### 3.5 Rectangular Waveguides

Rectangular waveguides are hollow metallic tubes of rectangular shape. Other types of waveguides are circular waveguides and coaxial waveguides. The electromagnetic waves in the waveguide are reflected from the the walls and travel in the longitudinal direction. The frequency band of a waveguide is given by the physical size of the tube. The long side of the waveguide opening is denoted  $a$  and the short side is denoted  $b$ . This is illustrated in figure 3.7.

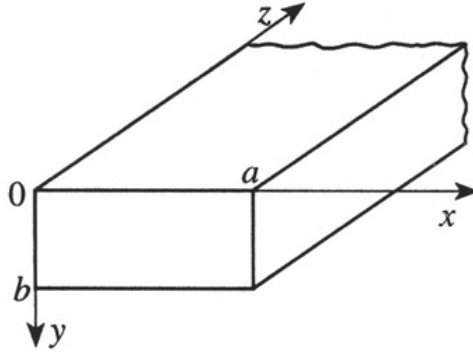


**Figure 3.7:** Waveguide dimensions.

The cutoff frequency for a rectangular waveguide is given by:

$$f_{c_{mn}} = \frac{1}{2\pi\sqrt{\mu\epsilon}} \sqrt{\left(\frac{m\pi}{a}\right)^2 + \left(\frac{n\pi}{b}\right)^2} \quad (3.46)$$

where  $m$  and  $n$  are the mode numbers in the  $x$  and  $y$  direction respectively.

For the fundamental  $TE_{10}$ -mode the equation is simplified to:

$$f_{c_{10}} = \frac{1}{2a\sqrt{\mu\epsilon}} \quad (3.47)$$

**Table 3.2:** Frequency band vs. rectangular cross section dimensions (a x b).

Designation	Dimensions (Inches)	Freq. Band (GHz)	Cutoff Freq. (GHz)
WR284	2.840 x 1.340	2.60 - 3.95	2.078
WR159	1.590 x 0.795	4.90 - 7.05	3.711
WR90	0.900 x 0.400	8.20 -12.4	6.557
WR75	0.750 x 0.375	10.0 - 15.0	7.868
WR51	0.510 x 0.255	15.0 - 22.0	11.571

Table 3.2 show cut-off frequencies for common waveguides.

For waveguides in general the wave impedance in the guide will vary with frequency. However, the impedance will be the same in the entire waveguide. The wave impedance can be calculated based on the cut-off frequency for the waveguide where the impedance is dependent on the polarization of the field in the guide. Equation 3.48 and 3.49 give the formulas for TE and TM modes respectively:

$$Z = \frac{Z_0}{\sqrt{1 - \left(\frac{f_c}{f}\right)^2}} \quad (3.48)$$

$$Z = Z_0 \sqrt{1 - \left(\frac{f_c}{f}\right)^2} \quad (3.49)$$

## 3.6 Calibration

Automatic network analyzers (ANAs) are widely used to measure the scattering parameters for passive and active devices. This is done by measuring scattering parameters as complex voltage amplitude ratios (Pozar, 2011). However the ANA has to be calibrated before the measurements are done. For a two-port measurement of a DUT two *error boxes* are defined on either side of the DUT. These *error boxes* include the loss, delay and other imperfections of the cables, connections, adapters etc. By doing this the reference plane is moved from somewhere inside the ANA to the face of the DUT. Figure 3.8 show a block diagram illustrating the *error boxes* on either side of the DUT.

A simple and often used way to calibrate an ANA is to use known loads (Pozar, 2011). The SOLT calibration method use a Short, Open, Load and Through to determine the scattering parameters of the *error boxes*. The problem with using known loads for calibration lies in the fact that the loads always are imperfect and introduce errors in the measurement (Pozar, 2011).

Another calibration method is the Thru-Reflection-Line (TRL) calibration method. Instead of predefined loads this method is based on three connections which can be used to characterize the *error boxes*; *Thru, Reflection and Line*.

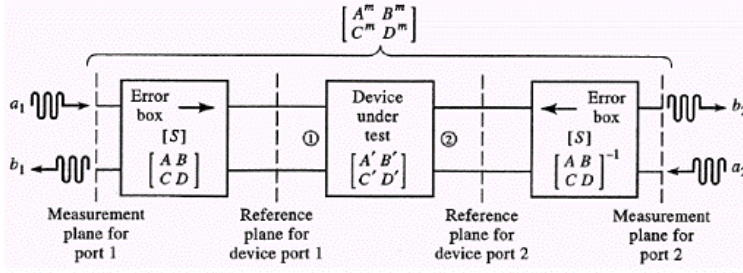


**Figure 3.8:** DUT with error boxes (Pozar, 2011).

The TRL-calibration is very useful when measuring scattering parameters in waveguides. The *Thru* connection is made by connecting the coax-to-waveguide-adapter of port 1 and port 2 respectively, the *Reflect* connection is made by mounting a plate covering the waveguide opening of port 1 and port 2 and the *Line* connection is made by mounting a length of waveguide between the waveguide adapter of port 1 and port 2. The S-parameters are recorded for each calibration component. The length of the *Line* connection can be calculated as follows (Baker-Jarvis et al., 2005):

The phase delay  $\Phi$  in a waveguide, the line length  $l$  and the wavelength  $\Lambda_g$  in the waveguide, given by equation 3.48, is related by:

$$l = \frac{\Phi \Lambda_g}{2\pi} \quad (3.50)$$

To find the *line* length calculate  $l$  for a phase delay of  $20^\circ$  at the lowest frequency of the sweep and a phase delay of  $160^\circ$  at the highest frequency of the sweep and choose a line length in between the two. This is typically  $\frac{\lambda}{4}$  at a geometric center frequency  $f_{center} = \sqrt{f_{min} f_{max}}$ .



---

# Design

## 4.1 Matlab

### 4.1.1 ABCD-Method

To calculate the total response of a radome sandwich material a script in Matlab using the ABCD-method described in section 3.4.2 has been written. For calculation of the transmission and reflection coefficients a set of parameters have to be defined before running the script. These parameters are described in table 4.1. The script is able to calculate up to 10 individual sandwich layers but additional layers can easily be added if needed. A flowchart of the calculation steps in the script is shown in figure 4.1.

**Table 4.1:** Matlab ABCD-script parameters.

Parameter	Description
N	Number of sandwich layers
fmin	Minimum simulation frequency
fmax	Maximum simulation frequency
Pol	Polarization of electric field. 1-Parallel (TM) and 2-Perpendicular (TE)
$Er_i$	Relative permittivity of the $i$ th layer
$t_i$	Thickness of the $i$ th layer
$tand_i$	Loss tangent of the $i$ th layer
$theta$	Incidence angle(s)

Figure 4.2, 4.3, 4.4 and 4.5 show reflection coefficients of different radome styles. For

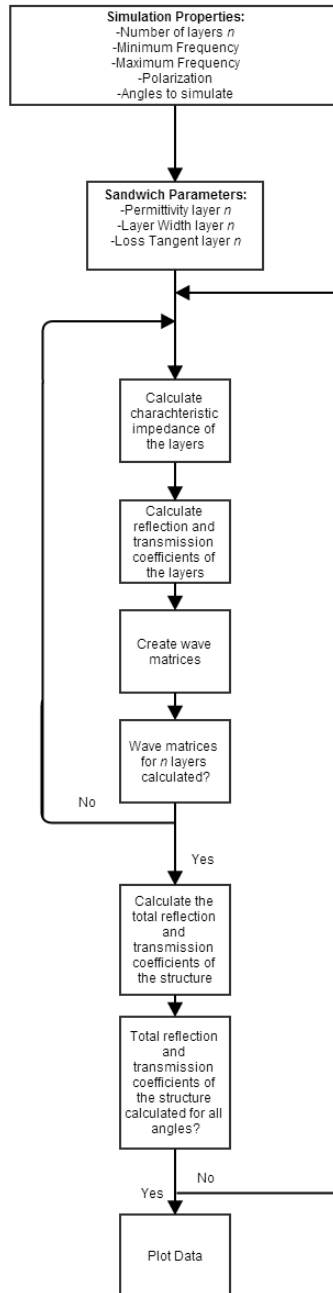


**Figure 4.1:** Flowchart for the Matlab ABCD script.

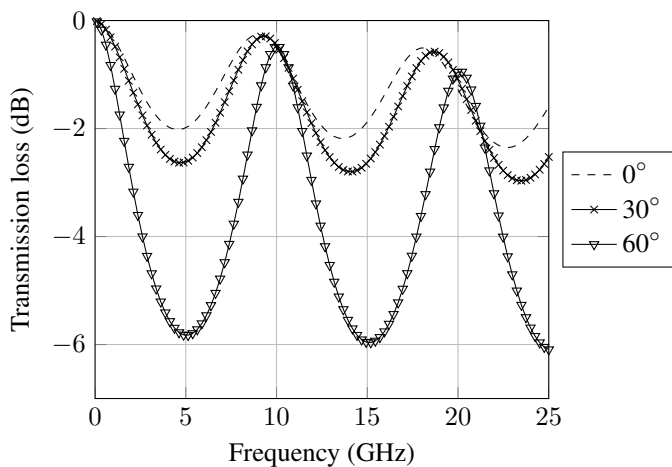


**Figure 4.2:** Half-wave wall transmission, perpendicular polarization ( $t = 0.8255\text{cm}$ ,  $\epsilon_r = 4$ ,  $\tan\delta = 0.015$ ).

verification of the script the plots have been made using the same material properties as figure 5.5, 5.10, 5.12 and 5.15 in Kozakoff (2010). A comparison of the plots from the Matlab script and the plots in Kozakoff (2010) show that the data are identical.

## 4.2 Matlab ABCD-Method Waveguide Compensation

The Matlab script described in subsection 4.1.1 calculate the transmission and reflection loss for transmission through a predefined radome sandwich material. When comparing the results from the script with measurements from the waveguide test setup modifications have to be done in order to achieve a correct result. Equation 3.40 and 3.41 are used by the script to calculate the impedance of the individual layers. However the two formulas are normalized for the wave impedance of free space:

$$Z_0 = \mu_0 c_0 = 4\pi \cdot 10^{-7} \text{H/m} \cdot 3 \cdot 10^8 \text{m/s} \approx 377\Omega \quad (4.1)$$

As described in 3.5 the wave impedance in a waveguide is dependent on the frequency. Equation 3.48 and 3.49 give the wave impedance for TE-modes and TM-modes respectively.

Because of the frequency dependency in the waveguide equation 3.40 and 3.41 has been modified to account for the impedance variation.

### 4.2.1 Optimization

Generally speaking, optimization is the process of finding the best values for some sort of function, sometimes within a set of bounds. The Matlab optimization-toolbox contains many different tools to solve different optimization problems, curve fitting and data fitting

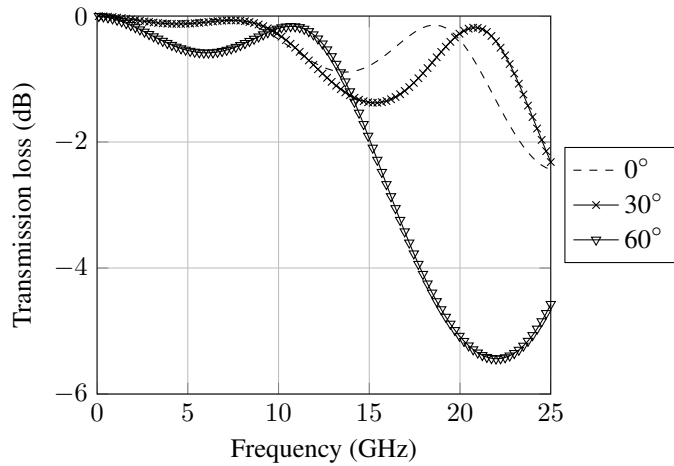


**Figure 4.3:** A-sandwich transmission, perpendicular polarization (skins:  $t = 0.0762\text{cm}$ ,  $\epsilon_r = 3.23$ ,  $\tan\delta = 0.016$ , core:  $t = 1.016\text{cm}$ ,  $\epsilon_r = 1.1$ ,  $\tan\delta = 0.001$ ).

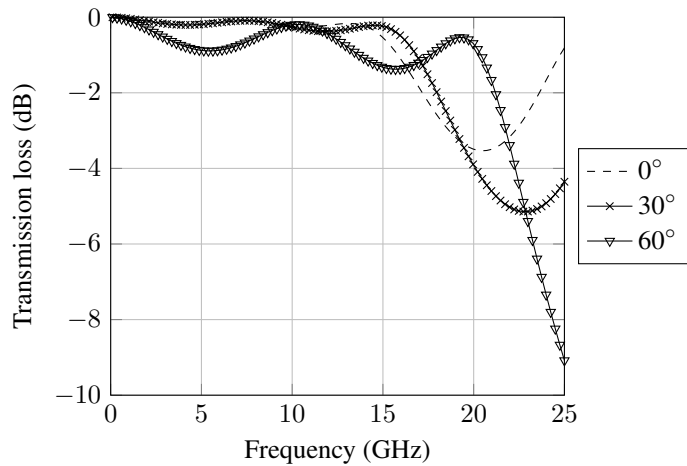


**Figure 4.4:** C-sandwich transmission, perpendicular polarization (skins:  $t = 0.0762\text{cm}$ ,  $\epsilon_r = 3.23$ ,  $\tan\delta = 0.016$ , cores:  $t = 0.5842\text{cm}$ ,  $\epsilon_r = 1.1$ ,  $\tan\delta = 0.001$ ).

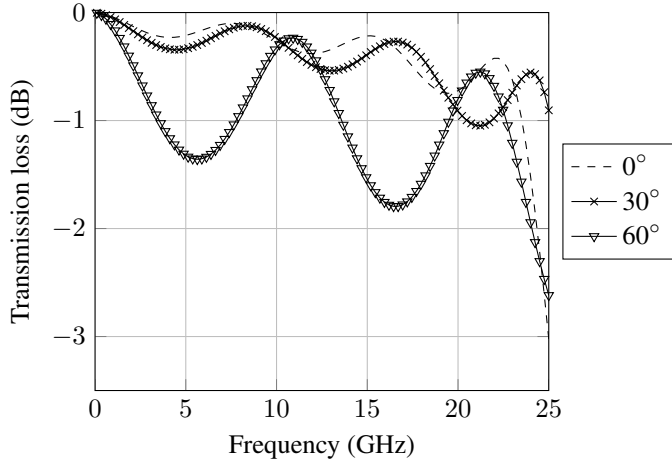


**Figure 4.5:** Seven-layer wall transmission, perpendicular polarization (skins:  $t = 0.0762\text{cm}$ ,  $\epsilon_r = 3.23$ ,  $\tan\delta = 0.016$ , cores:  $t = 0.3302\text{cm}$ ,  $\epsilon_r = 1.1$ ,  $\tan\delta = 0.001$ ).

including methods for linear, nonlinear and least squares fitting optimization, both constrained and unconstrained. The least squares fitting method is used in the matlab scripts that solve the optimization problem "Measured response versus simulated response" described later. Generally speaking an optimization process tries different parameter values in order to minimize the value of a defined error function. For instance in a curve fitting optimization, the error function would typically be the difference between a measured curve and a calculated one. The calculated curve is given by a function with parameters adjusted by the optimization process. To illustrate the advantage of the least square fitting method two parameters  $M_i$  and  $C_i$ , where  $M_i$  is the  $i$ th measured value and  $C_i$  is the  $i$ th calculated value, are defined. The error function for the measured curve versus the calculated curve can consequently be defined as:

$$E = \sum_{i=1}^n M_i - C_i \quad (4.2)$$

The problem with this error function is the scenario where the calculated curve have values below the measured curve. This will lead to a reduction in the error function even though the error might be larger than where the calculated curve have values above the measured one. To solve this problem the least square method square the error values and we get a new error function defined as:

$$E = \sum_{i=1}^n (M_i - C_i)^2 \quad (4.3)$$

By doing this the optimization process try to reduce the area of the sum of the error squares.

---

The *lsqnonlin* function is used to optimize the relative permittivity and loss tangent in order to match a simulated response with a measured response. *lsqnonlin* is a function that solve nonlinear least square problems of the form (Mathworks, 2013):

$$\min_x \| f(x) \|_2^2 = \min_x (f_1(x)^2 + f_2(x)^2 + \dots + f_n(x)^2) \quad (4.4)$$

However, *lsqnonlin* does not compute the sum of squares but the vector-valued function (Mathworks, 2013):

$$f(x) = \begin{bmatrix} f_1(x) \\ f_2(x) \\ \cdot \\ \cdot \\ f_n(x) \end{bmatrix} \quad (4.5)$$

The error values are therefore organized in a vector in the optimization scripts and the vector is used as the error function for the *lsqnonlin* function.

*lsqnonlin* is able to handle lower and upper bounds of the optimization parameters and this is an advantage when optimizing *relative permittivity* ( $\epsilon_r$ ) and *loss tangent* (*tand*) of the different sandwich layers since  $\epsilon_r$  always is larger than 1 (at optical frequencies, metals for instance may have a negative  $\epsilon_r$ , but that is not relevant for this thesis) and *tand* always is positive. This make the optimization process faster because the range of the optimized values are limited within a span of realistic values. The *lsqnonlin* function have a number of input parameters. The syntax used for the optimization problems in this thesis is: `x = lsqnonlin(fun, x0, lb, ub)`. The different arguments are described in table 4.2

**Table 4.2:** *lsqnonlin* input arguments.

Parameter	Description
x	Value of the error function
fun	Error function for sum of squares to be optimized
x0	Initial guess for x (possible to define an array of parameters $[x_0, x_1, \dots, x_n]$ )
lb	Lower boundary of the optimization parameters (possible to define an array of parameters $[lb_1, lb_2, \dots, lb_n]$ )
ub	Upper boundary of the optimization parameters (possible to define an array of parameters $[ub_1, ub_2, \dots, ub_n]$ )

*fminsearch* is a Matlab function that finds the minimum of multivariable functions (Mathworks, 2014). However, this function is designed for unconstrained optimization without lower and upper bounds for the variables. This is not ideal and a modified version of *fminsearch* named *fminsearchbnd* is used (D'Errico, 2012). This version accepts

variable boundaries which make it possible to avoid "invalid" values and speed up the optimization. For the frequency band transmission optimization the `fminsearchbnd` function has been used. Table 4.3 describe the input arguments of the function.

**Table 4.3:** `fminsearchbnd` input arguments.

Parameter	Description
x	Value of the error function
fun	Error function to be optimized
x0	Initial guess for x (possible to define an array of parameters $[x_0, x_1, \dots, x_n]$ )
lb	Lower boundary of the optimization parameters (possible to define an array of parameters $[lb_1, lb_2, \dots, lb_n]$ )
ub	Upper boundary of the optimization parameters (possible to define an array of parameters $[ub_1, ub_2, \dots, ub_n]$ )

### Measured Response versus Simulated Response

In order to match a simulated radome sandwich response with a measured response the Matlab script `Optimization.m` and `Wall_Transmission_Optimization.m` require a set of input parameters and S-parameter data from a measurement to perform a curve fitting optimization utilizing `lsqnonlin`.

Table 4.4 and table 4.5 show the different parameters and data required to do the optimization.

**Table 4.4:** `Optimization.m` input arguments.

Parameter	Description
$[Er1, Er2, \dots, Ern]$	Initial relative permittivity of layer n
$[tand1, tand2, \dots, tandn]$	Initial dielectric loss tangent for layer n
$[lb1, lb2, \dots, lbn]$	Lower boundary for layer n
$[ub1, ub2, \dots, ubn]$	Upper boundaries for layer n

### Frequency Band Transmission Optimization

The Matlab scripts `Optimization_Frequency_Band.m` and `Wall_Transmission_Optimization_Frequency_Band.m` optimize the thickness of the individual layers in order to maxi-



---

**Table 4.5:** *Wall\_Transmission\_Optimization.m* input parameters and data.

<b>Parameter</b>	<b>Description</b>
N	Number of sandwich layers
fmin	Minimum simulation frequency
fmax	Maximum simulation frequency
S11	S11 values from waveguide measurement
S21	S21 values from waveguide measurement

mize the transmission in one or more frequency bands. The two scripts require the input parameters described in table 4.6 and table 4.7. This optimization routine use the *fmin-searchbnd*-algorithm to find the minimum transmission loss for one- or several frequency bands.

**Table 4.6:** *Optimization\_Frequency\_Band.m* input parameters and data.

<b>Parameter</b>	<b>Description</b>
$[thickness1, thickness2, \dots, thicknessn]$	Initial thickness for layer n
$[lb1, lb2, \dots, lbn]$	Lower boundary for layer n
$[ub1, ub2, \dots, ubn]$	Upper boundaries for layer n

**Table 4.7:** *Wall\_Transmission\_Optimization\_Frequency\_Band.m* input parameters and data.

<b>Parameter</b>	<b>Description</b>
N	Number of sandwich layers
fmin	Minimum simulation frequency
fmax	Maximum simulation frequency
z	Number of frequency bands to optimize for
f_optim_lown	Low frequency for band n
f_optim_highn	High frequency for band n

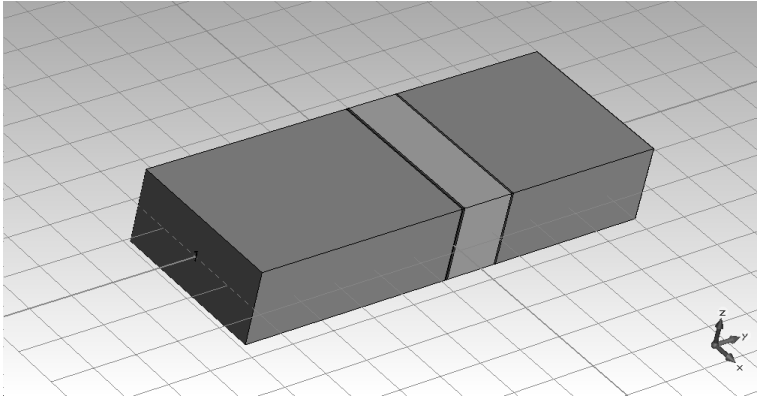


**Figure 4.6:** CST Microwave Studio simulation of WR284 waveguide with sandwich insert.

### 4.3 CST Microwave Studio

In order to have a better foundation for measurement verification the specimen measured in the waveguide setup has been simulated in CST Microwave Studio. The coax-to-waveguide adapter has also been designed and simulated in CST. CST is a 3D Electromagnetic simulation tool for high frequency components such as antennas, waveguides, coaxial lines and microstrip lines. CST lets the user define simulation boundaries, physical material properties, electrical properties, ports, probes, simulation frequency span and simulation method. The results are presented in both 2D-plots, Smith-Chart and 3D-animations of the electric- and magnetic fields. For this particular simulation, S-parameter results are of interest.

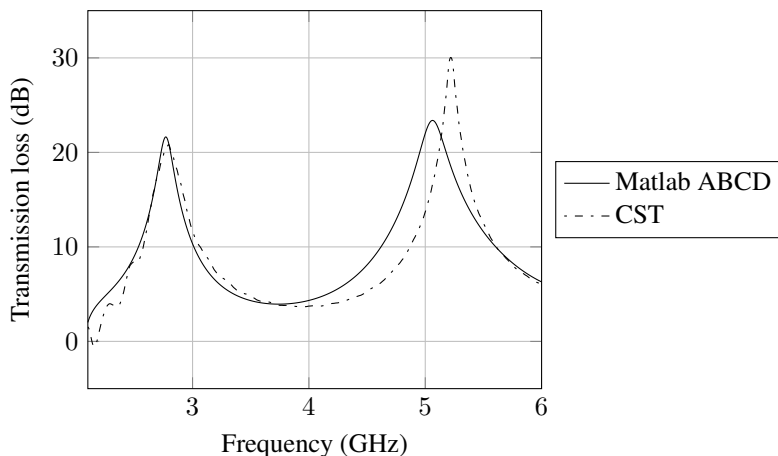
Figure 4.6 show the waveguide with the sandwich insert in CST. The waveguide is made by defining a "vacuum box" inside a perfect electrical conductor (PEC), the different sandwich layers are defined and placed inside the box and waveguide ports are defined at both ends of the waveguide.

Figure 4.7 show a comparison between a simulation in Matlab and CST. The Matlab data have been generated using the modified ABCD-method script which accounts for the frequency dependent impedance variations in the waveguide.

### 4.4 Waveguide Measurement Setup

#### 4.4.1 Waveguide Measurement and Calibration Kit Design

To design and produce drawings for the waveguide measurement setup and the TRL calibration kit CST Microwave studio has been used. The waveguide measurement setup consists of two Waveguide to SMA adapters and a specimen holder. The waveguide parts were manufactured by the mechanical workshop locally at the Department of Electronics and Telecommunications.



**Figure 4.7:** Comparison between ABCD-simulation in Matlab and simulation in CST Microwave Studio. (layer 1:  $t = 3.0\text{cm}$ ,  $\epsilon_r = 1.08$ ,  $\tan\delta = 0.001$ , layer 2:  $t = 4.0\text{cm}$ ,  $\epsilon_r = 3.8$ ,  $\tan\delta = 0.001$ ).

### Coax-to Waveguide Adapter

When designing a coaxial to waveguide adapter two parameters have to be calculated; the length of the coax probe exciting the electric field inside the waveguide and the distance from the coax probe to the backwall of the adapter. This is illustrated in figure 4.8. As seen in the figure tuning screws have been installed to fine tune the frequency response after determining the distance from the backwall and the probe length. This is not implemented in the designed coax-to-waveguide adapter.

To determine the best placement and length of the coax probe the adapter was optimized in CST. Two ports were defined; port 1 was defined at the waveguide-flange-plane and port 2 was defined at the coaxial connector. After defining the ports a 2-port optimization was run where the goal was to minimize S11 over the frequency band  $2.6 - 4\text{GHz}$ . The optimized values are displayed in table 4.8. Figure 4.9 and 4.10 show the optimized values for S11 and S21. At center frequency, 3.3 GHz S11 is approximately  $-22\text{dB}$  and S21  $-0.04\text{dB}$ .

**Table 4.8:** Coax-to-Waveguide design parameters.

Parameter	Length (mm)
Overall length of adapter	150
Distance from backwall	22.5
Probelength (inside waveguide)	18.5
Cross section (a,b)	72.14, 34.04

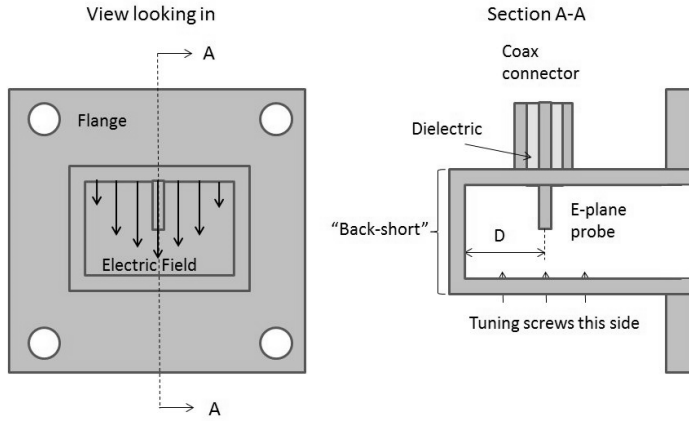


**Figure 4.8:** SMA to waveguide adapter design parameters (Microwaves101, 2013).

### Through, Reflect, Line Calibration Components and Sample Holder

The calibration components were designed in accordance with the method described in Baker-Jarvis et al. (2005). The through component was realized by connecting the two coax-to-waveguide adapters to each other. However, when performing the calibration on the test setup it is important that the sample holder is connected throughout the entire calibration process. If the calibration was done without the sample holder installed the reference plane would be shifted after reconnection of this component.

The reflection component of the TRL-calibration kit is a "plate" which is mounted between the two SMA-to-Waveguide adapters (actually between adapter number 1 at one side and the sample holder connected to adapter number 2 at the other side). The manufactured reflection component is illustrated in figure 4.12.

The line component was designed in accordance with the procedure described in section 3.6.

The cut-off frequency for a WR284 waveguide is 2.078 GHz as shown in table 3.2 and the corresponding cut-off wavelength is 0.144m. To calculate the length of the line-component equation 3.50 was used. The waveguide wavelength  $\lambda_g$  was calculated for a low frequency (3.1 GHz) and a high frequency (3.5 GHz):

$$\lambda_g = \frac{\lambda}{\sqrt{1 - \left(\frac{\lambda}{\lambda_c}\right)^2}} \quad (4.6)$$

$$\lambda_{g,3.1} = 0.1305m \quad (4.7)$$

$$\lambda_{g,3.5} = 0.1066m \quad (4.8)$$

Then the line length for the two frequencies were calculated:

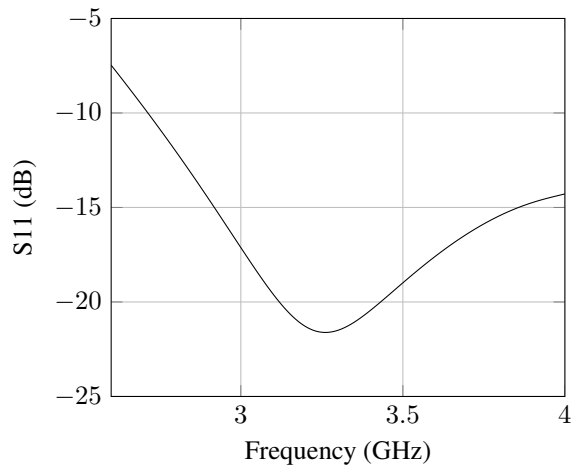


**Figure 4.9:** S11 for SMA to waveguide adapter.

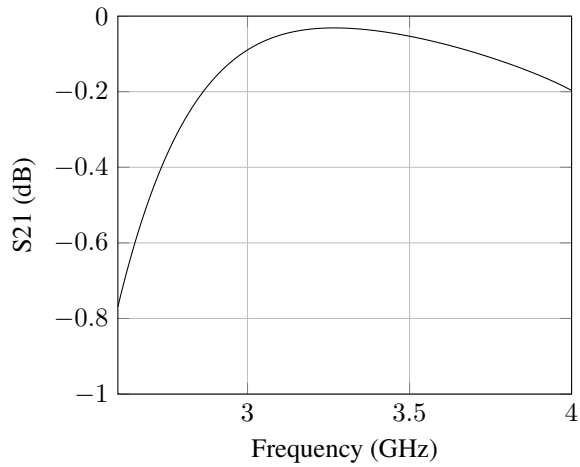


**Figure 4.10:** S21 for SMA to waveguide adapter.

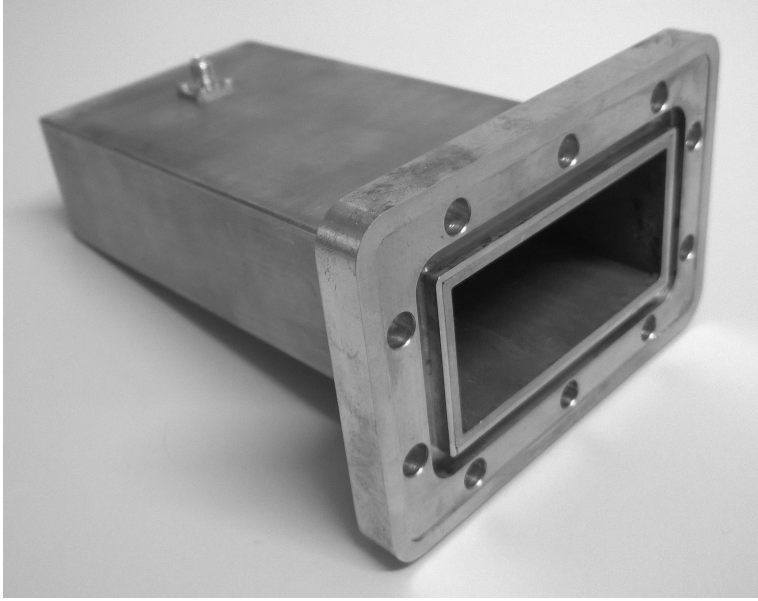


**Figure 4.11:** SMA to waveguide adapter.

$$\phi = 20^\circ = 0.349rad \quad (4.9)$$

$$l_1 = \frac{0.349 \cdot 0.1305}{2\pi} = 0.00725m \quad (4.10)$$

$$\phi = 160^\circ = 2.793rad \quad (4.11)$$

$$l_2 = \frac{2.793 \cdot 0.1066}{2\pi} = 0.0474m \quad (4.12)$$

Finally the length of the line component was found:

$$l = \frac{0.00725 + 0.0474}{2} = 0.0273m \quad (4.13)$$

The sample holder was designed as a 5 cm long waveguide tube with flanges to connect it to the SMA-to-Waveguide adapters. The component is shown in figure 4.14. The length of this component is not critical, the only requirement is that the holder is longer than the thickness of the sample to be measured.

### Calibration

The calibration of the test setup was done using the built-in features of the ANA. The ANA used for the calibration procedure and measurements is an *Agilent Technologies E8364B*.

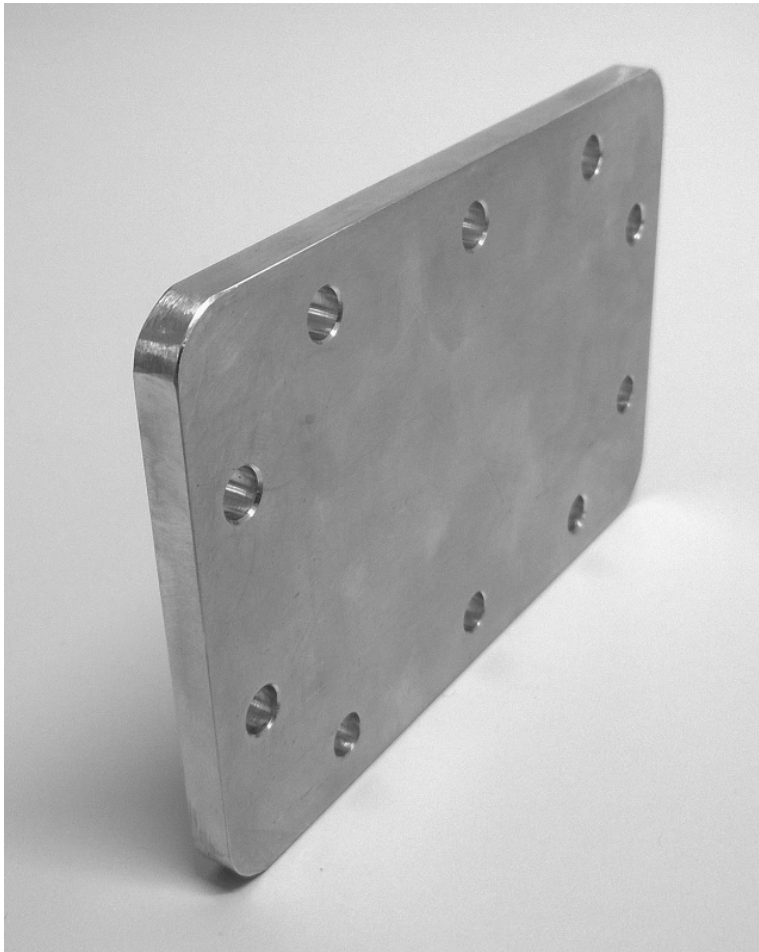


**Figure 4.12:** Reflection component for TRL calibration kit.

The 2-port TRL-calibration process is done using the calibration interface on the ANA. The transmission, reflection and line S-parameters are measured stepwise and a calibration set is calculated. The S-parameter values before and after calibration is presented in chapter 5. Figure 4.15 show the GUI on the ANA during calibration.

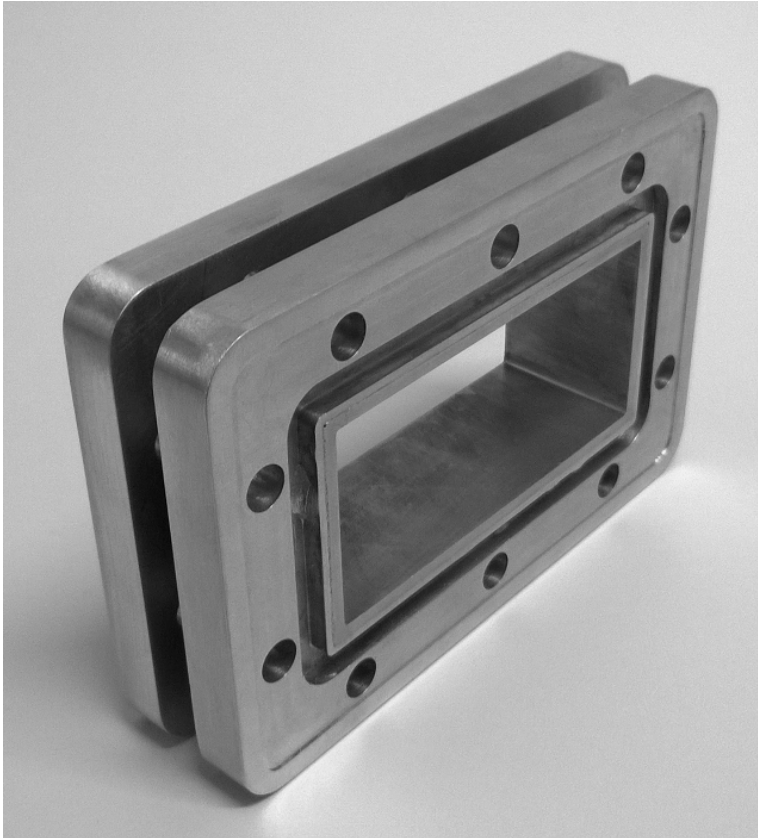


**Figure 4.13:** Line component for TRL calibration kit.



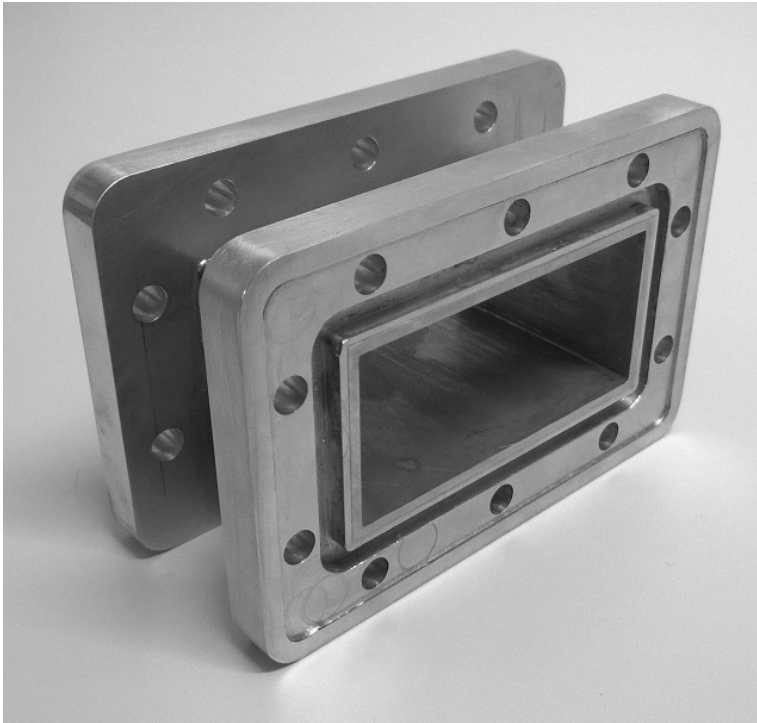


**Figure 4.14:** Sample holder for waveguide measurement setup.



**Figure 4.15:** Through, reflect, line calibration on ANA.

# Measurements and Results

## 5.1 Waveguide Measurements

### 5.1.1 Calibration

The calibration of the waveguide test setup was done according to the procedure described in section 3.6. Figure 5.1 and 5.2 show a comparison of S11 and S21 for the test setup before and after calibration. The measurements were done with an empty sample holder.

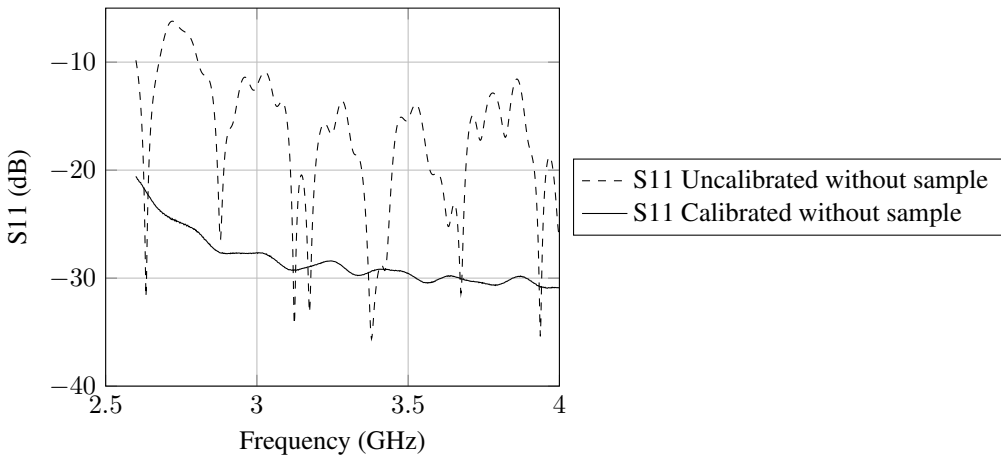


**Figure 5.1:** Uncalibrated S11 values versus calibrated S11 values, empty waveguide.

### 5.1.2 Radome Sandwich Sample

After calibrating the waveguide test setup a sample of radome sandwich material was measured. The individual layer properties are presented in table 5.1. Figure 5.3 and 5.4

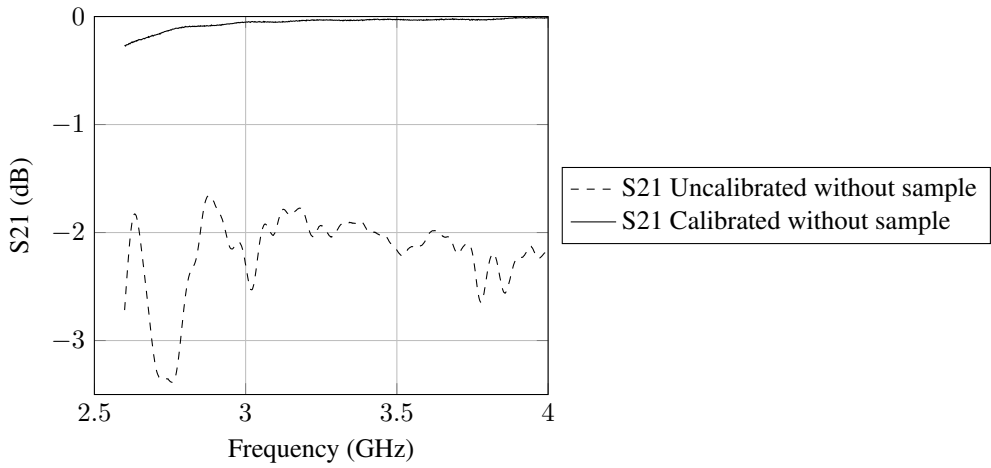


**Figure 5.2:** Uncalibrated S21 values versus calibrated S21 values, empty waveguide.

illustrate the sample and the sample inserted in the waveguide sample holder.

**Table 5.1:** Material properties for the measured sandwich sample.

Layer	Thickness (mm)	$\epsilon_r$	$\tan \delta$
Gelcoat	0.5	2.9	0.01
Laminate	0.9	3.8	0.001
Core	24	1.08	0.001
Laminate	0.9	3.8	0.001

Figure 5.5 show the complete test setup assembled and connected to the ANA.

The measurement data from the complete sandwich and the individual layers are presented in figure 5.6.

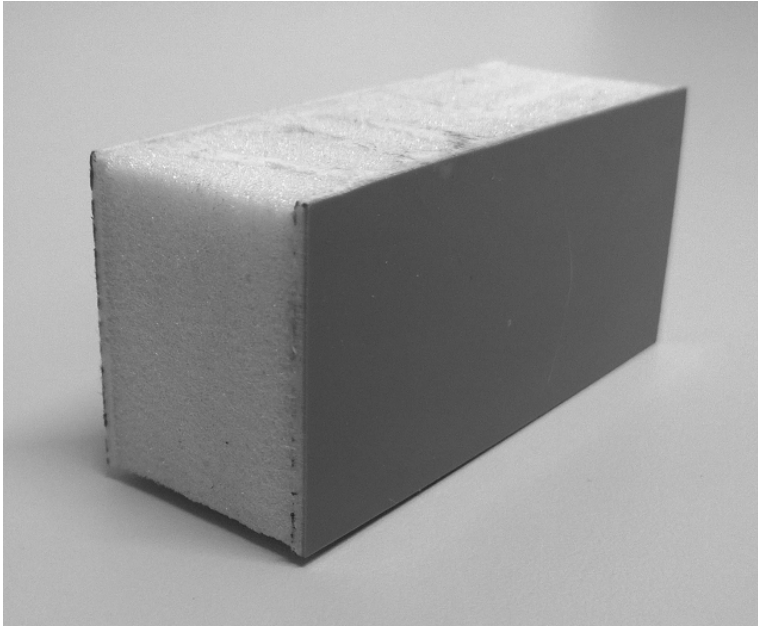


**Figure 5.3:** Radome sandwich sample cut to inner waveguide dimensions.



**Figure 5.4:** Radome sandwich sample inserted in sample holder.

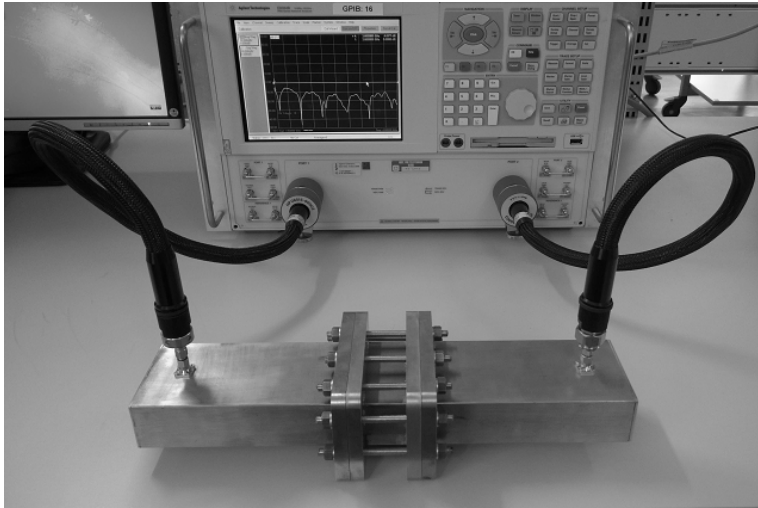


**Figure 5.5:** Waveguide measurement test setup and ANA.

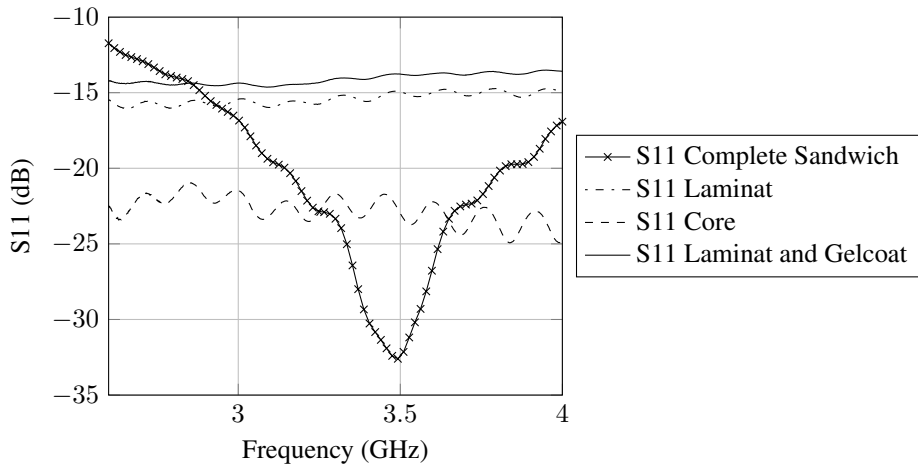


**Figure 5.6:** Measured S11 values from complete radome sandwich and the individual layers.

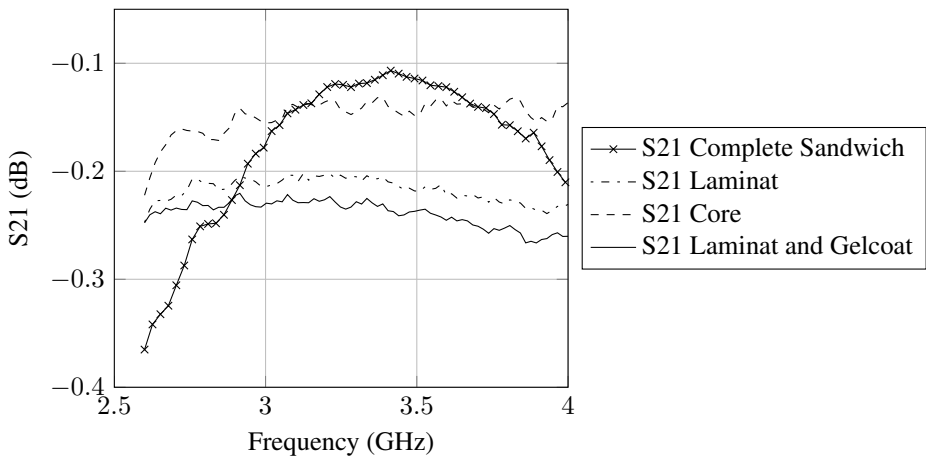


**Figure 5.7:** Measured S<sub>21</sub> values from complete radome sandwich and the individual layers.

---

### 5.1.3 Sample Gap

After measuring a sandwich sample completely filling the cross section of the waveguide sample holder two smaller samples were measured to test the effect of a gap between the sample and the sample holder. The electrical field strength is larger at the long sides of the waveguide cross section and the presumption is that a gap at one or both of the long sides will have a greater effect on the measurement results than a gap at one or both of the short sides. Two samples were made with a 5 mm gap on the long side and the short side respectively. As shown in figure 5.8 a larger deviation was measured with a gap at the long sides. This result was expected and emphasize the importance of preparing a sandwich sample which completely fills the cross section of the waveguide with minimum gap between the sample and the waveguide walls.

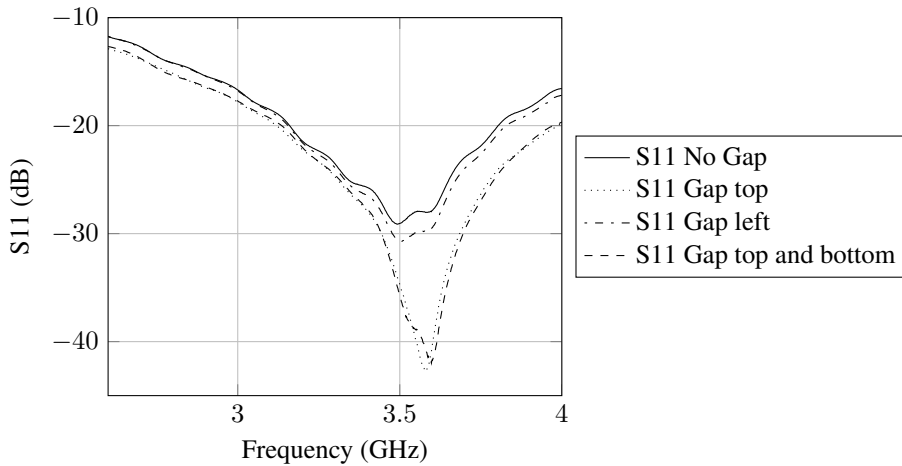


**Figure 5.8:** Comparison between the S11 values for a radome sandwich element with different gaps between sample and waveguide.

## 5.2 Optimization Results

### 5.2.1 Measured Response versus Simulated Response

After measuring the radome sandwich material, the individual layers of the sandwich and a sample of FR4 substrate were measured in the waveguide setup and the S-parameter data were exported to Matlab. After formatting the data the optimization scripts described in section 4.2.1 were run. The results from the optimizations are presented in table 5.2.

The figures from 5.9a to 5.16b show comparisons between the measured and simulated reflection- and transmission loss for the materials given in table 5.2.

**Table 5.2:** Optimization results for measured response values versus simulated response. Values marked with \* indicate that the upper/lower bound of the optimization was reached.

Material	Initial $\epsilon_r$	Optimized $\epsilon_r$	Initial $\tan \delta$	Optimized $\tan \delta$
Radome sandwich	$\epsilon_{r1,i} = 2.9$	$\epsilon_{r1,o} = 2.81$	$\tan \delta_{1,i} = 0.01$	$\tan \delta_{1,i} = 0.0134$
	$\epsilon_{r2,i} = 3.8$	$\epsilon_{r2,o} = 4.18$	$\tan \delta_{2,i} = 0.001$	$\tan \delta_{2,i} = 0.0377$
	$\epsilon_{r3,i} = 1.08$	$\epsilon_{r3,o} = 1.01$	$\tan \delta_{3,i} = 0.001$	$\tan \delta_{3,i} = 0.0005^*$
	$\epsilon_{r4,i} = 3.8$	$\epsilon_{r4,o} = 4.27$	$\tan \delta_{4,i} = 0.001$	$\tan \delta_{4,i} = 0.0005^*$
Core	$\epsilon_{r1,i} = 1.08$	$\epsilon_{r1,o} = 1.19$	$\tan \delta_{1,i} = 0.001$	$\tan \delta_{1,i} = 0.01$
Gelcoat - Laminat	$\epsilon_{r1,i} = 2.9$	$\epsilon_{r1,o} = 3.07$	$\tan \delta_{1,i} = 0.01$	$\tan \delta_{1,i} = 0.074$
	$\epsilon_{r2,i} = 3.3$	$\epsilon_{r2,o} = 4.99^*$	$\tan \delta_{2,i} = 0.001$	$\tan \delta_{2,i} = 0.0583$
FR4 Substrate	$\epsilon_{r1,i} = 4.4$	$\epsilon_{r1,o} = 4.82$	$\tan \delta_{1,i} = 0.02$	$\tan \delta_{1,i} = 0.1^*$

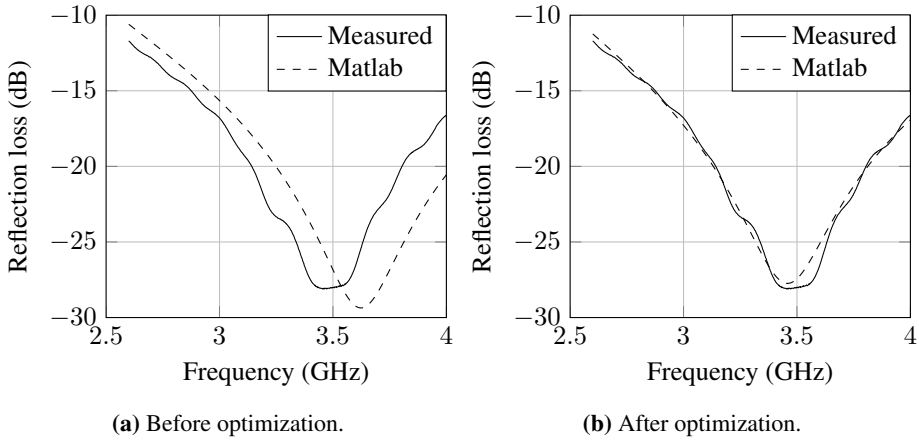


**Figure 5.9:** Comparison between the measured and simulated reflection coefficients before and after optimization of the relative permittivity and loss tangent for the radome sandwich sample



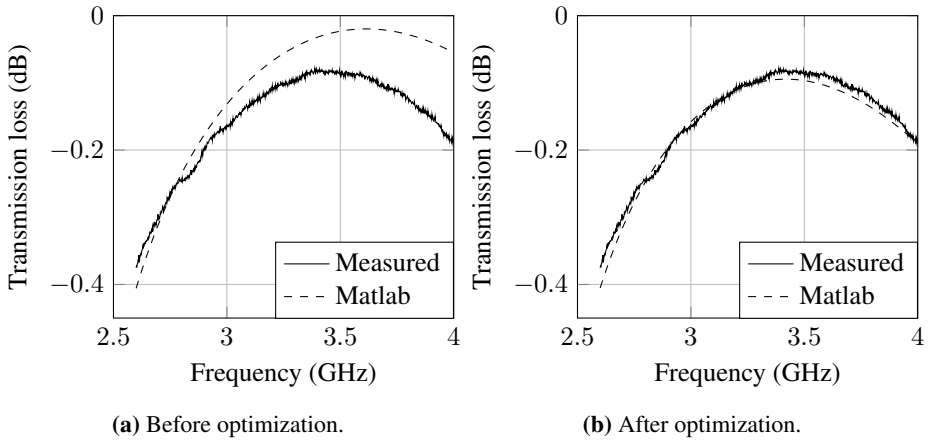


**Figure 5.10:** Comparison between the measured and simulated transmission coefficients before and after optimization of the relative permittivity and loss tangent for the radome sandwich sample.

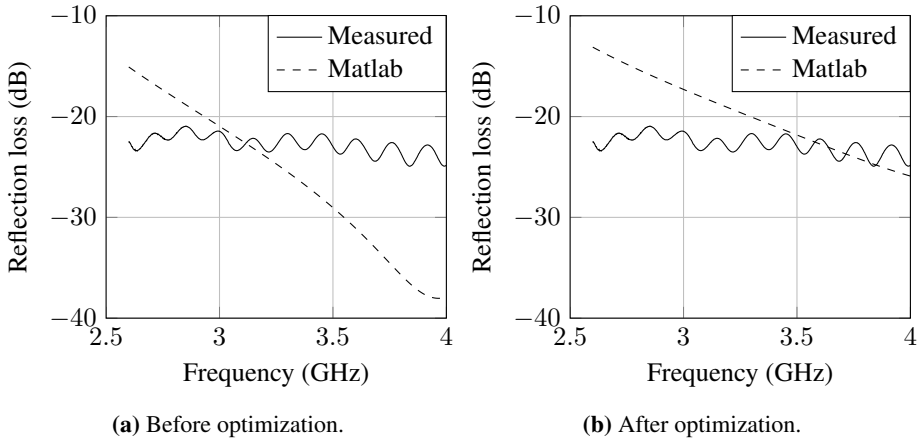


**Figure 5.11:** Comparison between the measured and simulated reflection coefficients before and after optimization of the relative permittivity and loss tangent for the core layer of the radome sandwich sample.

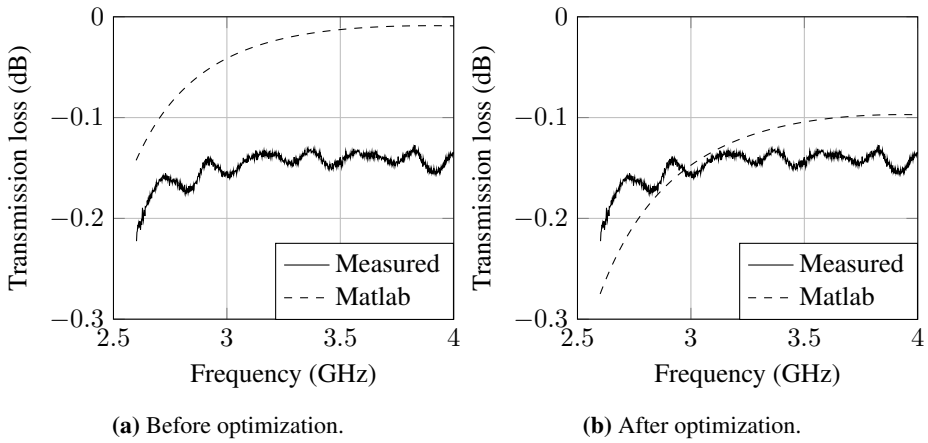


**Figure 5.12:** Comparison between the measured and simulated transmission coefficients before and after optimization of the relative permittivity and loss tangent for the core layer of the radome sandwich sample.

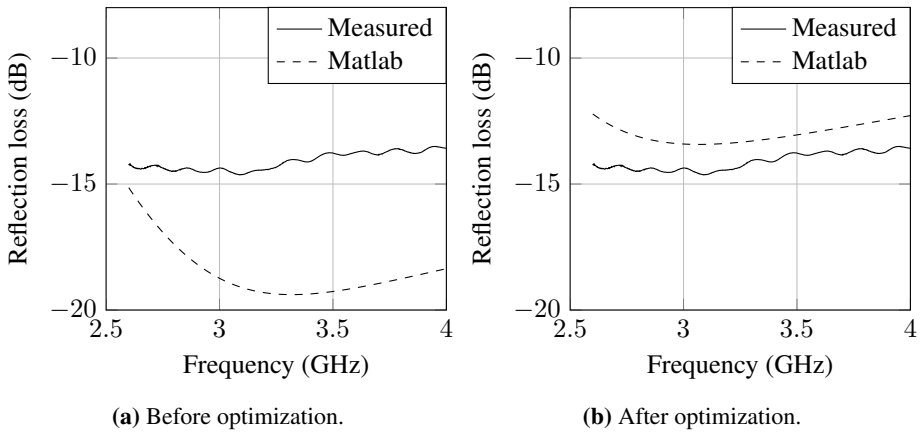


**Figure 5.13:** Comparison between the measured and simulated reflection coefficients before and after optimization of the relative permittivity and loss tangent for the laminate and gelcoat layer of the radome sandwich sample.

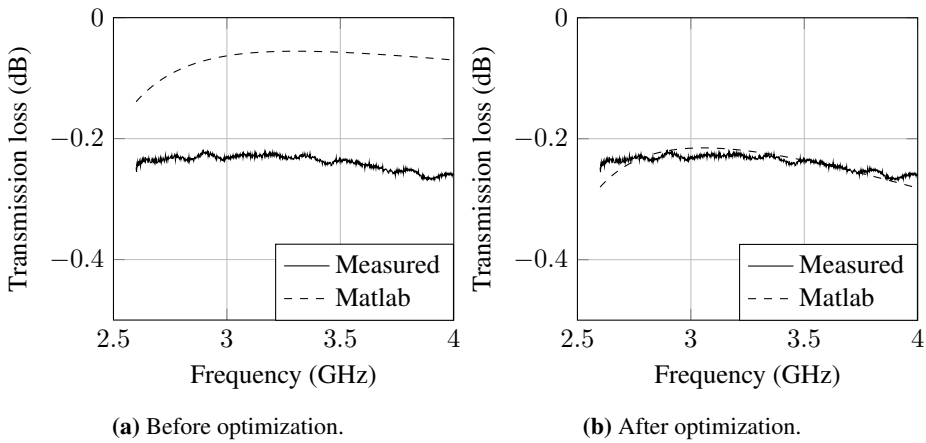


**Figure 5.14:** Comparison between the measured and simulated transmission coefficients before and after optimization of the relative permittivity and loss tangent for the laminate and gelcoat layer of the radome sandwich sample.

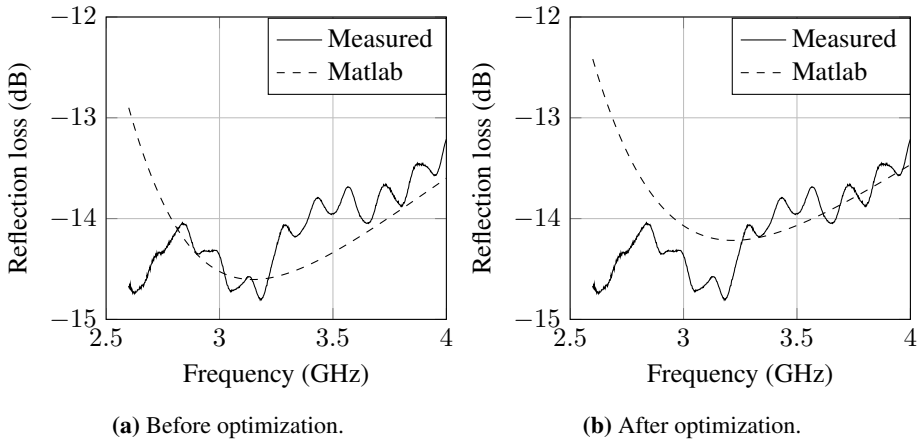


**Figure 5.15:** Comparison between the measured and simulated reflection coefficients before and after optimization of the relative permittivity and loss tangent for a sample of FR4 substrate.

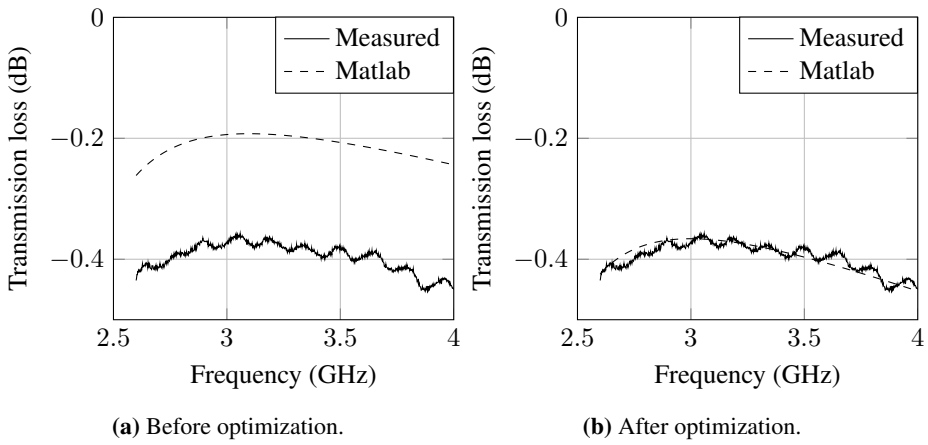


**Figure 5.16:** Comparison between the measured and simulated transmission coefficients after optimization of the relative permittivity and loss tangent for a sample of FR4 substrate.

## 5.2.2 Frequency Band Transmission Optimization

As described in subsection 4.2.1 two scripts have been written in Matlab in order to adjust one- or more radome layer thicknesses. The purpose is to maximize transmission through the material at one or more predefined frequency band(s). Table 5.3 show results from three different optimizations.

**Table 5.3:** Optimization results for transmission at given frequency band(s).

Material	Frequency band	Optimized thickness
Half-Wave Wall, $\epsilon_r = 3$ , $\tan \delta = 0.01$	8 – 12 GHz	$t_o = 8.3\text{mm}$
Half-Wave Wall, $\epsilon_r = 3$ , $\tan \delta = 0.01$	14 – 16 GHz	$t_o = 5.7\text{mm}$
A-Sandwich, $\epsilon_{r,core} = 1.1$ , $\tan \delta_{core} = 0.001$	7 – 8 GHz & 18 – 19 GHz	$t_o = 10.2\text{mm}$

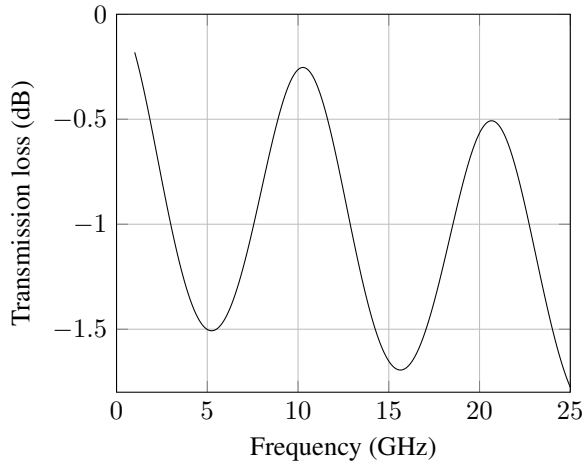


**Figure 5.17:** Transmission loss coefficient for a 1 layer Half-wave wall optimized for 8 – 12GHz (X-band).

The results presented in table 5.3 are ideal results. From a production point of view however, one always have to account for production variations. The thickness of the individual layers will vary causing a frequency shift of the transmission loss. Figure 5.20 show a comparison between the transmission loss of the A-sandwich from table 5.3 with optimized thickness of the core and two samples were the thickness has been changed with

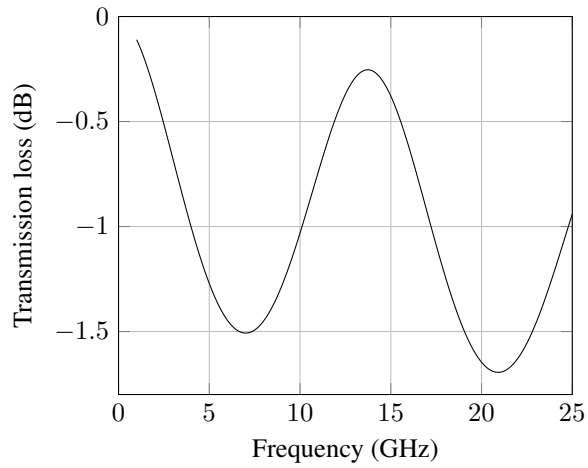


**Figure 5.18:** Transmission loss coefficient for a 1 layer Half-wave wall optimized for 14 – 16GHz.

$\pm 10\%$  from the optimized value. Table 5.4 show the frequency deviation in percent for 8-12 GHz and 19-20 GHz.

**Table 5.4:** Frequency band deviation with  $\pm 10\%$  thickness deviation.

Frequency band	Frequency deviation (%)
7 – 8 GHz	7.2%
19 – 20 GHz	10.2%

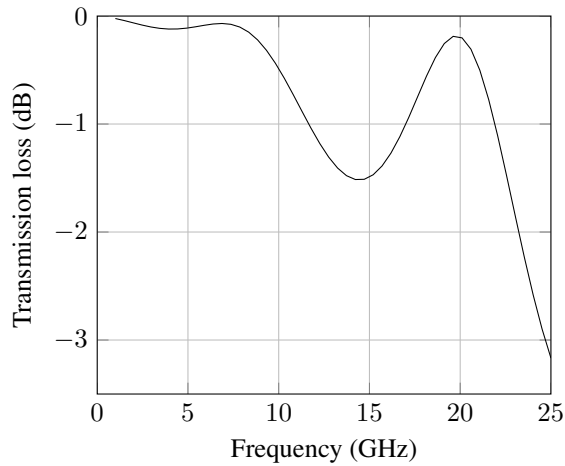


**Figure 5.19:** Transmission loss coefficient for a 3 layer A-sandwich optimized for 7 – 8GHz and 18 – 19GHz.

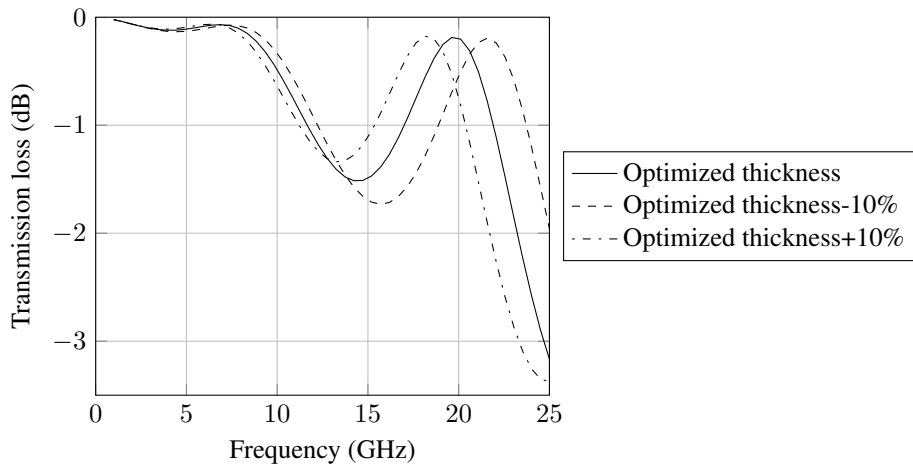


**Figure 5.20:** Comparison of the transmission loss for an A-sandwich with optimized thickness of the core, 10% reduced thickness of the core and 10% increased thickness of the core.

# Analysis

## 6.1 Matlab ABCD-script

Comparison of the simulated transmission and reflection coefficients generated by *Wall-transmission.m* and data from Kozakoff (2010) show that the script is working correctly. However the script is only correct for free space simulations. For design purposes this is fine but for comparison between simulated data and data measured from a waveguide test setup the script has been modified to take into account the frequency dependent wave impedance in a waveguide. The equations on which the script is based upon are normalized to the wave impedance of free space. In order to adjust the impedance the equations have been modified to include the frequency dependent impedance in the waveguide. Figure 4.7 show a comparison between Matlab and CST Microwave studio after implementation of the impedance adjustments. As seen from the plot the values correspond better for the lower part of the frequency band than for the higher where the peak value is approximately 6 dB lower and shifted from approximately 5.2 GHz to 5.05 GHz.

## 6.2 Waveguide TRL and Measurement Components

The waveguide measurement results presented in chapter 5 show that the components described in chapter 4 work as intended. The drawback using a waveguide based test system is the limited bandwidth of rectangular waveguides. The WR284 waveguide supports electromagnetic waves from 2.6 - 3.95 GHz. The size of the waveguide was chosen because the measured sandwich material is designed for a radar operating in S-band (2-4 GHz). As described later in section 6.3 the low frequency of the measurements is a problem when measuring thin materials. Choosing a smaller waveguide standard would allow for higher frequencies to be used in the measurements and thus increase the accuracy of the measurements.



---

### 6.3 Matlab versus Measurement Results

A high degree of similarity between the simulation results from Matlab and the waveguide measurement results is crucial in order to compute the actual permittivity and dielectric loss tangent of the samples. The optimization routines depend on the simulation- and measurement results in order to find the electrical properties of the sandwich layers. If the deviation between the two methods is too large the optimized values will be inaccurate.

There are several sources of error which could explain deviation between the simulation- and measurement results. Firstly, the thickness of the individual layers have to be correct. Before the measurements were performed the thickness of the layers were measured using a digital caliper. Especially for the individual sandwich layers, the correct thickness was difficult to measure. In lack of layer samples a complete sandwich sample was split. The splitting was done with a scalpel and it was difficult to separate the layers without affecting the thickness and the surface roughness. For the FR4 substrate the copper had to be sanded off before the measurement. Because traces of metal on the substrate would lead to a high reflection coefficient the substrate had to be ground a little extra in order to be certain that all the metal was removed. Because of the initial sample thickness of 1.6 mm a rough surface will affect the measurements more than for a thick sample. Figure 6.1 illustrate the dependence of the computed permittivity on the thickness error. For a relative thickness error of 5% the relative permittivity error is approximately 8-9% and the dielectric loss error is approximately 15%.

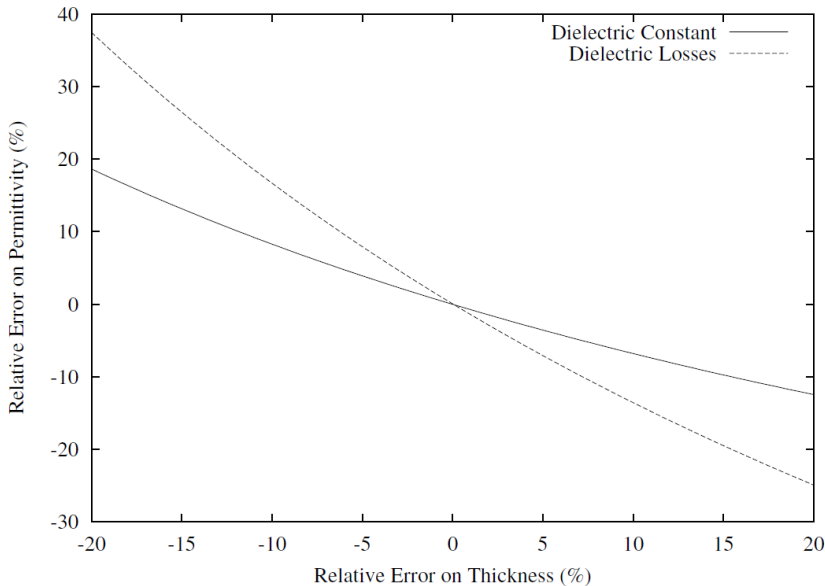


**Figure 6.1:** Dependence of the computed permittivity on the thickness error (Olmí et al., 2002).

Secondly, an air gap between the sample and the waveguide walls will affect the measurement. This is discussed and illustrated in subsection 5.1.3. However the sandwich

---

samples were precisely machined and the fit inside the waveguide sample holder was good. It is therefore assumed that the effect from an eventual air gap is neglectable.

The calibration of the waveguide measurement setup is also a source of error. However, the calibration results were good with S11 below 25dB for most of the band. This result indicate that the calibration dit not influence the measurements in a large degree.

When a waveguide is excited both the fundamental  $TE_{10}$  mode and higher order modes will be present close to the exciting probe. However the higher order modes are evanescent and after traveling a distance in the waveguide only the fundamental mode will propagate in the guide. In the waveguide test setup a sample of sandwich material is placed inside the waveguide sample holder. As the waves propagate through the individual sandwich layers some of the energy is reflected and some of it is transmitted. When this happens higher order modes will be excited. If the individual layers are thin the higher order modes will propagate to the next layer and affect the measurements.

The optimization results presented in table 5.2 show the permittivity and loss tangent values, before and after optimization. Table 6.1 display the difference between the measured and optimized values. From the results it can be seen that the number of layers, the permittivity and the thickness of the material is affecting the end result. Thicker materials with low permittivity have a better initial match between simulation and measurement. This can be seen by looking at the optimization result for the core material. This material have a thickness of 24mm and a permittivity of 1.08. The results from the optimization also show that the optimized dielectric loss tangent values are varying. Abbas et al. (2001) describe results from complex permittivity measurements at Ka-band (26.5-40 GHz). The authors of the article conclude that the sample thickness is the most important factor for accurate permittivity and dielectric loss tangent calculations. The samples used in the measurements were in the order of 4-14 mm. At 26.5-40 GHz the respective wavelengths are 11.3-7.5 mm. An earlier article from the same authors, Abbas et al. (1998), came to the same conclusion that  $\Delta\epsilon_r$  increase with narrower samples. The article also show lower  $\Delta\epsilon_r$  for materials with low-loss. For the measurements in this thesis the wavelengths are 115.4-75.0 mm and the thickness of the samples vary between 0.5-26.5 mm.

From table 6.1 it is evident that the optimized loss tangent values are inaccurate at best. The main reasons for the deviation are the initial difference between the measured and simulated values and the thickness of the samples relative to the wavelength. Because of the deviation between the measured and simulated transmission and reflection coefficients the optimizer have to adjust the permittivity and loss tangent values more in order to fit the data sets.

In addition to the deviation of the measurements compared to the simulations the thickness of the samples measured are very thin relative to the wavelength. As a consequence a small degree of attenuation have to be registered by the ANA. Also the materials in the sandwich radome are low loss materials which make it even more difficult to register the loss.

The combination of the inaccuracy of the measurement- and simulation results together with the thickness of the samples explain the large degree of deviation between initial and optimized values, especially for the dielectric loss tangent.

Two samples of Teflon (PTFE) were measured for verification of the measurement setup and the optimization routine, and to investigate the effect of samples with different

**Table 6.1:** Optimization results for measured response values versus simulated response. Values marked with \* indicate that the upper/lower bound of the optimization was reached.

<b>Material</b>	$\Delta\epsilon_r$	$\Delta\epsilon_r$ %	$\Delta \tan \delta$	$\Delta \tan \delta$ %
Radome	0.09	3.1%	0.0034	34%
sandwich	0.38	10.0%	0.0367	3670%
	0.07	6.5%	0.0005*	50%
	0.47	12.4%	0.0005*	50%
Core	0.11	10.2%	0.009	900%
Gelcoat -	0.17	5.9%	0.064	640%
Laminat	1.69	44.4%	0.0573	5730%
FR4 Substrate	0.42	9.5%	0.08	800%

thicknesses. The Teflon samples have well defined dielectric properties and make them ideal for this measurement. The relative permittivity of Teflon is  $\epsilon_r = 2.1$  and the dielectric loss tangent is  $\tan \delta = 0.0002$ . Two samples were measured with a thickness of 11mm and 22mm respectively. Table 6.2 show the optimized permittivity and loss tangent results. Because of the low loss of Teflon the loss tangents were not optimized as their values proved to have little or no effect on the optimization results. The optimization results show that the thicker sample have a more accurate permittivity value than the more narrow sample. This supports the conclusions from Abbas et al. (1998) and Abbas et al. (2001).

**Table 6.2:** Permittivity and loss tangent Teflon (PTFE). The loss tangents were not optimized as their values proved to have little or no effect on the optimization results.

<b>Thickness</b>	$\epsilon_r$	$\Delta\epsilon_r$	$\tan \delta$
11.0mm	2.39	13.6%	0.0002*
22.0mm	2.13	1.4%	0.0002*

## 6.4 Matlab Script for Frequency Band Optimization

The frequency band optimization scripts are based upon the matlab script *Wall\_transmission.m*. The results from the optimization scripts shows that the optimization is working as expected with low transmission loss figures for the predefined frequency bands. Figure 5.20 show a comparison of the transmission loss for an A-sandwich material where the optimized core thickness have been adjusted  $\pm 5\%$ . The plot shows that the error is larger for higher frequencies than for lower ones. This imply that the design tolerance is smaller

---

for radomes designed for higher frequencies. This is no surprise since the thickness error relative to the wavelength is larger at higher frequencies.

---

---

# Conclusion

## 7.1 Matlab Simulations

Comparison between the results computed by the *Wall\_Transmission.m*-script and simulation data from Kozakoff (2010) confirm that the script is working correctly. The script allows for transmission- and reflection coefficient computation for TE and TM waves for different incidence angles and frequencies. In its current state the program allows the user to simulate 10 different layers although additional layers can easily be implemented.

## 7.2 Waveguide Measurement and Calibration Components

In order to conduct measurements on different radome materials a waveguide test setup and a TRL-calibration kit has been designed and constructed. The measurement results show that the test setup work is working as intended. However, because of the waveguide standard used (WR284), accurate measurements of thin materials with low loss proved difficult. The results from the measurement of a complete radome sandwich sample show good correlation compared to simulations from CST Microwave Studio but measurements of the individual layers proved difficult.

## 7.3 Matlab Optimization

Two optimization scripts have been written using functions included in Matlab. The first optimization script, *Optimization.m* adjust the relative permittivity and loss tangent values of the individual sandwich layers in order to match the response from a measured- and simulated radome sample using least square optimization. The results reveal that the accuracy of the optimized relative permittivity values depend on the thickness of the test sample. For a 22 mm thick sample of Teflon the optimized value deviated with 1.3% from the specified permittivity value. With decreasing thickness of the test samples the deviation increased to approximately 3-12%. The optimized loss tangent values however show

---

very large deviation from the specified values. Various reasons for the inaccurate results are discussed in chapter 6 but the main reasons seem to be the low loss of the materials measured combined with the thickness of the layers relative to the wavelength of the measurements.

The second optimization script, *Optimization\_frequency\_band.m*, use the Matlab function *fminsearchbnd.m* in order to minimize the transmission loss for predefined frequency bands. This is done by adjusting the thickness of the core material(s) of a sandwich structure. The optimization results show that the script works correctly and is able to calculate values for one- and several frequency band(s). Adjustment of the optimized thickness with  $\pm 10\%$  has been done in order to investigate the effects of production errors. The result show a larger deviation for high frequencies.

## Future Work

Because of the problems experienced with accurate determination of the dielectric properties of the measured samples, especially for the loss tangent, it would be interesting to investigate the effect on the measurements if the measurement frequencies were increased. This would require a new set of waveguide test- and calibration to be designed and manufactured. However, these parts will in reality be "scaled down" versions of the parts described in this thesis.

For the Matlab scripts a GUI would be a big advantage if the scripts were to be used by someone without good knowledge to Matlab and programming. For the optimization scripts a routine to import S-parameter data from the measurements would ease the preparation of an optimization between a measured and simulated response. It would also be interesting to investigate the effect of the error function which is optimized. In its current state the error function is simply a sum of the deviation between the two curves point by point. Improving this could lead to better optimization results.



---

---

# Bibliography

- Abbas, Z., Pollard, R., Kelsall, R., 1998. A rectangular dielectric waveguide technique for determination of permittivity of materials at w-band. *IEEE Transactions on microwave theory and techniques* 46 (12), 2011–2015.
- Abbas, Z., Pollard, R., Kelsall, R., 2001. Complex permittivity measurements at ka-band using rectangular dielectric waveguide. *IEEE Transactions on instrumentation and measurement* 50 (5), 1334–1342.
- ASTM International, 2008. Standard Test Method for Measuring Relative Complex Permittivity and Relative Magnetic Permeability of Solid Materials at Microwave Frequencies Using Waveguide. ASTM International.
- Baker-Jarvis, J., Janezic, M., Riddle, B., Johnk, R., Kabos, P., Holloway, C., Geyer, R., Grosvenor, C., 2005. Technical Note 1536: Measuring the Permittivity and Permeability of Lossy Materials: Solids, Liquids, Metals, Building Materials, and Negative-Index Materials. National Institute of Standards and Technology, U.S. Department of Commerce.
- Collin, R., 1991. *Field Theory of Guided Waves*, 2nd Edition. John Wiley & Sons, Inc.
- D’Errico, J., 2012.  
URL <http://www.mathworks.com/matlabcentral/fileexchange/8277-fminsearchbnd--fminsearchcon>
- Kedar, A., Revankar, U., 2006. Parametric study of flat sandwich multilayer radome. *Progress in Electromagnetics Research* 66, 253–265.
- Kozakoff, D., 2010. *Analysis of Radome-Enclosed Antennas*, 2nd Edition. Artech House.
- Mathworks, 2013.  
URL <http://www.mathworks.se/help/optim/ug/lsgnonlin.html>
- Mathworks, 2014.  
URL <http://www.mathworks.se/help/matlab/ref/fminsearch.html>

---

Microwaves101, 2013.

URL [http://www.microwaves101.com/content/Waveguide\\_to\\_coax\\_transitions.cfm](http://www.microwaves101.com/content/Waveguide_to_coax_transitions.cfm)

MIL-R-7705B, 1988. Military specification radomes general specifications for.

Olmi, R., Tedesco, M., Ignesti, A., 2002. Thickness-independent measurement of the permittivity of thin samples in the x band. *Measurement Science and Technology* 13 (4), 503–509.

Peres, L., de Souza, C., Bonatti, I., Yook, J.-G., 2004. ABCD matrix: an unique tool for linear two-wire transmission line modelling.

Pozar, D., 2011. *Microwave Engineering*, 4th Edition. John Wiley & Sons, Inc.

Tereschenko, O., Buesink, F., Leferink, F., 2011. Measurement of complex permittivity of composite materials using waveguide method. *Proceedings of the 10th International Symposium on Electromagnetic Compatibility (EMC Europe 2011)* 10, 52–56.

Venkatesh, M. S., Raghavan, G. S. V., 2005. An overview of dielectric properties measuring techniques.

Virone, G., Tascone, R., Olivieri, A., Addamo, G., Peverini, O., 2007. A waveguide/free-space measurement setup for panels and joints of large dielectric radomes. *Proc. Int. Conf. Electromagn. Adv. Appl.*, Turin, Italy, Sep. 17–21, 792–794.

Wegner, E., Lobue, N., 1964. Electrical design and performance evaluation of dual-frequency radome test panels. *Proceedings of the OSU-RTD Symposium on Electromagnetic Windows* 5, 1–23.

---

# Appendix

## Appendix A - Wall\_Transmission.m

```
#####  
%SANDWICH RADOME SIMULATION  
#####  
  
%INPUT DATA  
  
%SIMULATION PROPERTIES  
clear;  
clc;  
N = 3;           %Number of layers  
fmin= 0.1;       %Minimum Frequency (GHz)  
fmax= 25;        %Maximum Frequency (GHz)  
pol= 2;          %Polarization Type Parallel(Tm) (1), Perpendicular(Te) (2)  
theta= [0 30 60]; %Angles to simulate  
  
%Constants  
E0=8.85e-12;  
Mu0=12.5664e-7;  
c=1/sqrt(E0*Mu0);  
  
%SANDWICH PARAMETERS  
  
%Layer 1  
Ei(1)= 4; %Permittivity  
t(1)= 0.8255e-2; %Layer Thickness (m)  
tand(1)= 0.015; %Loss tangent  
  
%Layer 2  
Ei(2)= 1.08; %Permittivity  
t(2)= 24e-3; %Layer Thickness (m)  
tand(2)= 0.001; %Loss tangent  
  
%Layer 3  
Ei(3)= 3.8; %Permittivity  
t(3)= 0.9e-03; %Layer Thickness (m)  
tand(3)= 0.001; %Loss tangent  
  
%Layer 4  
Ei(4)= 1.1; %Permittivity  
t(4)= 0.3302e-2; %Layer Thickness (m)
```

---

```

tand(4)= 0.001; %Loss tangent

%Layer 5
Ei(5)= 3.23; %Permittivity
t(5)= 0.0762e-02; %Layer Thickness (m)
tand(5)= 0.016; %Loss tangent

%Layer 6
Ei(6)= 1.1; %Permittivity
t(6)= 0.3302e-2; %Layer Thickness (m)
tand(6)= 0.001; %Loss tangent

%Layer 7
Ei(7)= 3.23; %Permittivity
t(7)= 0.0762e-2; %Layer Thickness (m)
tand(7)= 0.016; %Loss tangent

%Layer 8
Ei(8)= 1.1; %Permittivity
t(8)= 0.3302e-2; %Layer Thickness (m)
tand(8)= 0.001; %Loss tangent

%Layer 9
Ei(9)= 3.23; %Permittivity
t(9)= 0.0762e-2; %Layer Thickness (m)
tand(9)= 0.016; %Loss tangent

%Layer 10
Ei(10)= 1; %Permittivity
t(10)= 1; %Layer Thickness (m)
tand(10)= 1; %Loss tangent

%Free Space Layer (Do not alter)
Ei(N+1)= 1; %Permittivity
t(N+1)= 100000; %Layer Thickness (m)
tand(N+1)= 0; %Loss tangent

f=linspace(fmin,fmax,50); %Matrix with simulation frequencies
thetaradian=theta.*(pi/180); %Angle of incidence (Radian)

    sintheta=sin(thetaradian);
    costheta=cos(thetaradian);

for m=1:length(theta)
    sintheta1=sintheta(m);
    costheta1=costheta(m);

    %Total reflection and transmission coefficients
    for k =1:length(f);
    Gamma=2*(pi/(c/(f(k)*1e9)));

```

---

---

```

    TotalMatrix=1;

    %Characteristic layer impedance
    for i=1:N+1
        Er(i)=Ei(i)*(1-(j*tand(i)));
        if pol==1
            Z(i)=sqrt(Er(i)-(sintheta1^2))/(Er(i)*costheta1);
        elseif pol==2
            Z(i)=costheta1/sqrt(Er(i)-(sintheta1^2));
        end
    end

    %Reflection and transmission for the different layers
    refl(1)=(Z(1)-1)/(Z(1)+1);
    trans(1)=sqrt(1-refl(1)^2);
    for i=2:N+1
        refl(i)=(Z(i)-Z(i-1))/(Z(i)+Z(i-1));
        trans(i)=sqrt(1-refl(i)^2);
    end

    %Wave matrix calculation
    for i =1:(N)
        M=exp(j*Gamma*t(i)*sqrt(Er(i)-(sintheta1^2)));
        Mc=exp(-j*Gamma*t(i)*sqrt(Er(i)-(sintheta1^2)));
        TotalMatrix=TotalMatrix*(1/trans(i))*[M,refl(i)*Mc;refl(i)*M,Mc];
    end

    %Total reflection and transmission coefficients of the structure
    TotalMatrix=1/trans(N+1)*TotalMatrix*[1 refl(N+1); refl(N+1) 1];
    reflection(k)=TotalMatrix(2,1)/TotalMatrix(1,1);
    transmission(k)=1/TotalMatrix(1,1);

end

Transabs=abs(transmission);
Reflabs=abs(reflection);
Transabsdb=mag2db(Transabs);
Reflabsdb=mag2db(Reflabs);

%Plot the transmission and reflection coefficients in dB:
figure(1)
style=['k--';'k-x';'k-v'];
plot(f,Transabsdb,style(m,1:3));
hold on
grid;
xlabel('Frequency (GHz)');
ylabel('Transmission loss (dB)');
legend('0^{\circ}','30^{\circ}','60^{\circ}','Location','EastOutside');

figure(2)
style=['k--';'k-x';'k-v'];
plot(f,Reflabsdb,style(m,1:3));
hold on
grid;
xlabel('Frequency (GHz)');

```

---

---

```
ylabel('Reflection loss (dB)');  
legend('0^{\circ}', '30^{\circ}', '60^{\circ}', 'Location', 'EastOutside');
```

```
end
```

---

## Appendix B - Wall\_Transmission\_Guide\_Impedance.m

```
#####  
%SANDWICH RADOME SIMULATION WITH IMPEDANCE COMPENSATION  
#####  
  
%INPUTS  
  
%Structure properties  
clear;  
clc;  
N = 4;           %Number of layers  
fmin= 2.6;       %Lower Frequency (GHz)  
fmax= 4;         %Higher Frequency (GHz)  
pol= 2;         %Parallel(Tm) (1), Perpendicular(Te) (2)  
  
%Load data for comparison  
%load('S11_DUT_SUBSTRAT.mat');  
%load('S21_DUT_SUBSTRAT.mat');  
%load('S12_DUT_SUBSTRAT.mat');  
%load('S22_DUT_SUBSTRAT.mat');  
%load('Freq.mat');  
  
% load('S11_2lag.mat');  
% load('S21_2lag.mat');  
% load('S12_2lag.mat');  
% load('S22_2lag.mat');  
% load('Freq_2lag.mat');  
  
%Load data from HFSS  
%load('S11_Irene.mat');  
%load('S21_Irene.mat');  
%load('freq_Irene.mat');  
  
%Load data from CST  
% load('S11_2lag.mat');  
% load('S21_2lag.mat');  
% load('Freq_2lag.mat');  
  
%Constants  
E0=8.85e-12;  
Mu0=12.5664e-7;  
c=1/sqrt(E0*Mu0);  
a=72.136e-3;  
b=34.036e-3;  
fco=2.078e9;  
lambda_co=c/fco;  
% S11_DUT_ABS=abs(S11_DUT);  
  
%Layer parameters  
%Layer 1  
Ei(1)= 4.4; %Permittivity
```



---

```

t(1)= 1.6e-03; %Layer Thickness (m)
tand(1)= 0.02; %Loss tangent

%Layer 2
Ei(2)= 1.08; %Permittivity
t(2)= 24e-03; %Layer Thickness (m)
tand(2)= 0.001; %Loss tangent

%Layer 3
Ei(3)= 3.8; %Permittivity
t(3)= 0.9e-03; %Layer Thickness (m)
tand(3)= 0.001; %Loss tangent

%Layer 4
Ei(4)= 2.9; %Permittivity
t(4)= 0.5e-3; %Layer Thickness (m)
tand(4)= 0.01; %Loss tangent

%Layer 5
Ei(5)= 1; %Permittivity
t(5)= 1000; %Layer Thickness (m)
tand(5)= 0.0; %Loss tangent

%Layer 6
Ei(6)= 1.1; %Permittivity
t(6)= 0.5842e-2; %Layer Thickness (m)
tand(6)= 0.001; %Loss tangent

%Layer 7
Ei(7)= 3.23; %Permittivity
t(7)= 0.0762e-2; %Layer Thickness (m)
tand(7)= 0.016; %Loss tangent

%Layer 8
Ei(8)= 1.1; %Permittivity
t(8)= 0.3302e-2; %Layer Thickness (m)
tand(8)= 0.001; %Loss tangent

%Layer 9
Ei(9)= 3.23; %Permittivity
t(9)= 0.0762e-2; %Layer Thickness (m)
tand(9)= 0.016; %Loss tangent

%Layer 10
Ei(10)= 1; %Permittivity
t(10)= 1; %Layer Thickness (m)
tand(10)= 1; %Loss tangent

%Free Space Layer (Do not alter)
Ei(N+1)= 1; %Permittivity
t(N+1)= 1000; %Layer Thickness (m)
tand(N+1)= 0; %Loss tangent

theta= [0];

f=linspace(fmin*1e9,fmax*1e9,801); %Frequency matrix
%f2=linspace(2.6e9,4e9,29); %Optional frequency matrix external data plots

```

---

---

```

thetaradian=theta.*(pi/180); %Angle of incidence (Radian)

    sintheta=sin(thetaradian);
    costheta=cos(thetaradian);

for m=1:length(theta)

    sintheta1=sintheta(m);
    costheta1=costheta(m);

%Calculate the total reflection and transmission coefficients
for k =1:length(f);
    lambda_freespace(k)=c/(f(k));
    Gamma=2*(pi/lambda_freespace(k));
    total=1;

    %Characateristic layer impedance
    Z_w(k)=(1/sqrt(1-((fco/f(k))^2)));
    Er(1)=Ei(1)*(1-(j*tand(1)));
    Z(1)=(costheta1/sqrt(Er(1)-(sintheta1^2)))/Z_w(k);
    for i=2:N+1
        Er(i)=Ei(i)*(1-(j*tand(i)));
        if pol==1
            Z(i)=(sqrt(Er(i)-(sintheta1^2)))/(Er(i)*costheta1)/Z_w(k);
        elseif pol==2
            Z(i)=(costheta1/sqrt(Er(i)-(sintheta1^2)))/Z_w(k);
        end
    end

    %Reflection and transmission for the different layers
    reflection(1)=(Z(1)-1)/(Z(1)+1);
    transmission(1)=sqrt(1-reflection(1)^2);
    %tao(1)=1+ro(1);
    for i=2:N+1
        reflection(i)=(Z(i)-Z(i-1))/(Z(i)+Z(i-1));
        transmission(i)=sqrt(1-reflection(i)^2);
        %tao(i)=1+ro(i);
    end

    %Wave matrix calculation
    for i =1:(N)
        A=exp(j*Gamma*t(i)*sqrt(Er(i)-(sintheta1^2)));
        Ac=exp(-j*Gamma*t(i)*sqrt(Er(i)-(sintheta1^2)));
        total=total*(1/transmission(i))*[A,reflection(i)*Ac;reflection(i)*A,Ac];
    end

    %Total reflection and transmission coefficients of the structure
    total=1/transmission(N+1)*total*[1 reflection(N+1); reflection(N+1) 1];
    reflection_loss(k)=total(2,1)/total(1,1);
    transmission_loss(k)=1/total(1,1);

end

```

---

---

```
Transabs=abs(transmission_loss);
Reflabs=abs(reflection_loss);
Transabsdb=-mag2db(Transabs);
Reflabsdb=-mag2db(Reflabs);

%Plot
figure(1)
plot(Freq,mag2db(abs(S21_DUT_SUBSTRAT)), 'k-.', f, -Transabsdb, 'k-');
hold on
grid on;
axis ([fmin*1e9 fmax*1e9 -0.8 -0.2])
xlabel('Frequency (GHz)');
ylabel('Reflection loss (dB)');
legend('Measured', 'Matlab', 'Location', 'EastOutside');

end
```

---

## Appendix C - Wall\_Transmission\_Optimization.m

```
#####
%TRANSMISSION AND REFLECTION THROUGH MULTILAYER DIELECTRIC WALLS
#####

function Error = ABCD(E)
%INPUTS

%Structure properties
%clear;
%clc;
N = 4;           %number of layers
fmin= 2.6;       %Minimum Frequency (GHz)
fmax= 4.0;       %Maximum Frequency (GHz)
pol= 2;          %Polarization Type Parallel(Tm) (1), Perpendicular(Te) (2)

%Constants
E0=8.85e-12;
Mu0=12.5664e-7;
c=1/sqrt(E0*Mu0);
a=72.136e-3;
fco=2.078e9;
lambda_co=c/fco;

%Load measurements data from file
load('S11_DUT1.mat');
load('S21_DUT1.mat');
load('S11_DUT1.mat');
load('S21_DUT1.mat');

%load('Freq_Irene.mat');
%load('S11_Irene.mat');
%load('S21_Irene.mat');

%S11=S11abslinear.';
%S12=S12abslinear.';
%S21=S21abslinear.';
%S22=S22abslinear.';

%Layer parameters

%Layer 1
Ei(1)= E(1); %Permittivity
t(1)= 0.9e-03; %Layer Thickness (m)
tand(1)= 0.001; %Loss tangent

%Layer 2
Ei(2)= E(2); %Permittivity
t(2)= 24e-03; %Layer Thickness (m)
tand(2)= 0.001; %Loss tangent

%Layer 3
Ei(3)= E(3); %Permittivity
t(3)= 0.9e-03; %Layer Thickness (m)
```

---

```

tand(3)= 0.001; %Loss tangent

%Layer 4
Ei(4)= E(4); %Permittivity
t(4)= 0.5e-3; %Layer Thickness (m)
tand(4)= 0.01; %Loss tangent

% %Layer 5
% Ei(5)= E(9); %Permittivity
% t(5)= 1000; %Layer Thickness (m)
% tand(5)= E(10); %Loss tangent
%
% %Layer 6
% Ei(6)= E(11); %Permittivity
% t(6)= 0.5842e-2; %Layer Thickness (m)
% tand(6)= E(12); %Loss tangent
%
% %Layer 7
% Ei(7)= E(13); %Permittivity
% t(7)= 0.0762e-2; %Layer Thickness (m)
% tand(7)= E(14); %Loss tangent
%
% %Layer 8
% Ei(8)= E(15); %Permittivity
% t(8)= 0.3302e-2; %Layer Thickness (m)
% tand(8)= E(16); %Loss tangent
%
% %Layer 9
% Ei(9)= E(17); %Permittivity
% t(9)= 0.0762e-2; %Layer Thickness (m)
% tand(9)= E(18); %Loss tangent
%
% %Layer 10
% Ei(10)= E(19); %Permittivity
% t(10)= 1; %Layer Thickness (m)
% tand(10)= E(20); %Loss tangent

%Free Space Layer (Do not alter)
Ei(N+1)= 1; %Permittivity
t(N+1)= 1000; %Layer Thickness (m)
tand(N+1)= 0; %Loss tangent

theta=[0];

f=linspace(fmin*1e9,fmax*1e9,801); %Matrix with simulation frequencies
thetaradian=theta.*(pi/180); %Angle of incidence (Radian)

for l=1:length(theta)
    sintheta(l)=sin(thetaradian(l));
    costheta(l)=cos(thetaradian(l));
end

for m=1:length(theta)

```

---

---

```

        sinthetal=sintheta(m);
        costhetal=costheta(m);
%Total reflection and transmission coefficients
for k =1:length(f);
    lambda_freespace(k)=c/(f(k));
    Gamma=2*(pi/lambda_freespace(k));
    TotalMatrix=1;

    %w(k)=2*pi*f(k)*1e9;

    %Calculate characteristic impedance of the layers
    Z_w(k)=(1/sqrt(1-((fco/f(k)))^2));
    Er(1)=Ei(1)*(1-(j*tand(1)));
    Z(1)=(costhetal/sqrt(Er(1)-(sinthetal^2)))/Z_w(k);
    for i=2:N+1
        Er(i)=Ei(i)*(1-(j*tand(i)));
        if pol==1
            Z(i)=sqrt(Er(i)-(sinthetal^2))/(Er(i)*costhetal)/Z_w(k);
        elseif pol==2
            Z(i)=(costhetal/sqrt(Er(i)-(sinthetal^2)))/Z_w(k);
        end
    end

    %Individual reflection and transmission coefficients of the layers
    refl(1)=(Z(1)-1)/(Z(1)+1);
    trans(1)=sqrt(1-refl(1)^2);
    for i=2:N+1
        refl(i)=(Z(i)-Z(i-1))/(Z(i)+Z(i-1));
        trans(i)=sqrt(1-refl(i)^2);
    end

    %Generating wave matrices
    for i =1:(N)
        M=exp(j*Gamma*t(i)*sqrt(Er(i)-(sinthetal^2)));
        Mc=exp(-j*Gamma*t(i)*sqrt(Er(i)-(sinthetal^2)));
        TotalMatrix=TotalMatrix*(1/trans(i))*[M,refl(i)*Mc;refl(i)*M,Mc];
    end

    %Total reflection and transmission coefficients of the structure
    TotalMatrix=1/trans(N+1)*TotalMatrix*[1 refl(N+1); refl(N+1) 1];
    reflection(k)=TotalMatrix(2,1)/TotalMatrix(1,1);
    transmission(k)=1/TotalMatrix(1,1);

end

    Transabs=abs(transmission);
    Reflabs=abs(reflection);
    Transabsdb=mag2db(Transabs);
    Reflabsdb=mag2db(Reflabs);

%Plot the transmission and reflection coefficients in dB:
    figure(1);
    plot(f/1e9,mag2db(abs(S11_DUT1)),'k-',f/1e9,Reflabsdb,'k--')
    grid on;
    xlabel('Frequency (GHz)');

```

---

---

```
ylabel('Reflection loss (dB)');
legend('Measured', 'Matlab', 'Location', 'EastOutside');

figure(2);
plot(f/1e9, mag2db(abs(S21_DUT1)), 'k-', f/1e9, Transabsdb, 'k--')
grid on;
xlabel('Frequency (GHz)');
ylabel('Transmission loss (dB)');
legend('Measured', 'Matlab', 'Location', 'EastOutside');

for a=1:length(f);
curve1(a)=(abs(S21_DUT1(a)));
curve2(a)=Transabs(a);
E1(a)=(curve1(a)-curve2(a));
curve3(a)=(abs(S11_DUT1(a)));
curve4(a)=Reflabs(a);
E2(a)=(curve3(a)-curve4(a));

end
end

ehandle=@Wall_Transmission_Optimization;
Error=(E1+E2);
```

---

## Appendix D - W.\_T.\_Optimization\_frequency\_band.m

```
#####  
%TRANSMISSION AND REFLECTION THROUGH MULTILAYER DIELECTRIC WALLS  
#####  
  
function Error = ABCD(E)  
  
%Simulation settings  
N = 1; %number of layers  
fmin= 1; %Minimum Frequency (GHz)  
fmax= 25; %Maximum Frequency (GHz)  
polarization= 2; %Polarization Type Parallel (Tm) (1), Perpendicular (Te) (2)  
  
%Optimization Parameters  
  
z=1; %Number of frequency bands  
  
f_optim_low1=14; %Low Frequency band 1 (GHz)  
f_optim_high1=16; %High Frequency band 1 (GHz)  
  
f_optim_low2=18; %Low Frequency band 2 (GHz)  
f_optim_high2=20; %High Frequency band 2 (GHz)  
  
f_optim_low3=14; %Low Frequency band 2 (GHz)  
f_optim_high3=15; %High Frequency band 2 (GHz)  
  
f_optim_low4=13; %Low Frequency band 2 (GHz)  
f_optim_high4=14; %High Frequency band 2 (GHz)  
  
f_optim_low5=10; %Low Frequency band 2 (GHz)  
f_optim_high5=11; %High Frequency band 2 (GHz)  
  
%Constant values  
E0=8.85e-12;  
Mu0=12.5664e-7;  
c=1/sqrt(E0*Mu0);  
a=72.136e-3;  
fco=2.078e9;  
lambda_co=c/fco;  
  
%Properties of the individual layers (uncomment the relevant layers)  
  
%Layer 1  
Ei(1)= 3.23; %Permittivity  
t(1)= E(1); %Layer Thickness (m)  
tand(1)= 0.016; %Loss tangent  
  
% %Layer 2  
% Ei(2)= 1.1; %Permittivity  
% t(2)= E(2); %Layer Thickness (m)  
% tand(2)= 0.001; %Loss tangent  
%  
% %Layer 3  
% Ei(3)= 3.23; %Permittivity
```



---

```

% t(3)= E(3); %Layer Thickness (m)
% tand(3)= 0.016; %Loss tangent
%
% %Layer 4
% Ei(4)= 2.9; %Permittivity
% t(4)= E(4); %Layer Thickness (m)
% tand(4)= 0.01; %Loss tangent

% %Layer 5
% Ei(5)= E(9); %Permittivity
% t(5)= 1000; %Layer Thickness (m)
% tand(5)= E(10); %Loss tangent
%
% %Layer 6
% Ei(6)= E(11); %Permittivity
% t(6)= 0.5842e-2; %Layer Thickness (m)
% tand(6)= E(12); %Loss tangent
%
% %Layer 7
% Ei(7)= E(13); %Permittivity
% t(7)= 0.0762e-2; %Layer Thickness (m)
% tand(7)= E(14); %Loss tangent
%
% %Layer 8
% Ei(8)= E(15); %Permittivity
% t(8)= 0.3302e-2; %Layer Thickness (m)
% tand(8)= E(16); %Loss tangent
%
% %Layer 9
% Ei(9)= E(17); %Permittivity
% t(9)= 0.0762e-2; %Layer Thickness (m)
% tand(9)= E(18); %Loss tangent
%
% %Layer 10
% Ei(10)= E(19); %Permittivity
% t(10)= 1; %Layer Thickness (m)
% tand(10)= E(20); %Loss tangent

%Free Space Layer
Ei(N+1)= 1; %Permittivity
t(N+1)= 1000; %Layer Thickness (m)
tand(N+1)= 0; %Loss tangent

theta= [0];

f=linspace(fmin*1e9, fmax*1e9, 50);
thetaradian=theta.*(pi/180);

%Calculate frequency band

if z==1
low1=floor((f_optim_low1*1e9-fmin*1e9)/(((fmax-fmin)*1e9)/length(f)));
high1=ceil((f_optim_high1*1e9-fmin*1e9)/(((fmax-fmin)*1e9)/length(f)));

elseif z==2
    low1=floor((f_optim_low1*1e9-fmin*1e9)/(((fmax-fmin)*1e9)/length(f)));

```

---

---

```
high1=ceil((f_optim_high1*1e9-fmin*1e9)/(((fmax-fmin)*1e9)/length(f)));  
  
low2=floor((f_optim_low2*1e9-fmin*1e9)/(((fmax-fmin)*1e9)/length(f)));  
high2=ceil((f_optim_high2*1e9-fmin*1e9)/(((fmax-fmin)*1e9)/length(f)));
```

```
elseif z==3
```

```
low1=floor((f_optim_low1*1e9-fmin*1e9)/(((fmax-fmin)*1e9)/length(f)));  
high1=ceil((f_optim_high1*1e9-fmin*1e9)/(((fmax-fmin)*1e9)/length(f)));  
  
low2=floor((f_optim_low2*1e9-fmin*1e9)/(((fmax-fmin)*1e9)/length(f)));  
high2=ceil((f_optim_high2*1e9-fmin*1e9)/(((fmax-fmin)*1e9)/length(f)));  
  
low3=floor((f_optim_low3*1e9-fmin*1e9)/(((fmax-fmin)*1e9)/length(f)));  
high3=ceil((f_optim_high3*1e9-fmin*1e9)/(((fmax-fmin)*1e9)/length(f)));
```

```
elseif z==4
```

```
low1=floor((f_optim_low1*1e9-fmin*1e9)/(((fmax-fmin)*1e9)/length(f)));  
high1=ceil((f_optim_high1*1e9-fmin*1e9)/(((fmax-fmin)*1e9)/length(f)));  
  
low2=floor((f_optim_low2*1e9-fmin*1e9)/(((fmax-fmin)*1e9)/length(f)));  
high2=ceil((f_optim_high2*1e9-fmin*1e9)/(((fmax-fmin)*1e9)/length(f)));  
  
low3=floor((f_optim_low3*1e9-fmin*1e9)/(((fmax-fmin)*1e9)/length(f)));  
high3=ceil((f_optim_high3*1e9-fmin*1e9)/(((fmax-fmin)*1e9)/length(f)));  
  
low4=floor((f_optim_low2*1e9-fmin*1e9)/(((fmax-fmin)*1e9)/length(f)));  
high4=ceil((f_optim_high2*1e9-fmin*1e9)/(((fmax-fmin)*1e9)/length(f)));
```

```
elseif z==5
```

```
low1=floor((f_optim_low1*1e9-fmin*1e9)/(((fmax-fmin)*1e9)/length(f)));  
high1=ceil((f_optim_high1*1e9-fmin*1e9)/(((fmax-fmin)*1e9)/length(f)));  
  
low2=floor((f_optim_low2*1e9-fmin*1e9)/(((fmax-fmin)*1e9)/length(f)));  
high2=ceil((f_optim_high2*1e9-fmin*1e9)/(((fmax-fmin)*1e9)/length(f)));  
  
low3=floor((f_optim_low3*1e9-fmin*1e9)/(((fmax-fmin)*1e9)/length(f)));  
high3=ceil((f_optim_high3*1e9-fmin*1e9)/(((fmax-fmin)*1e9)/length(f)));  
  
low4=floor((f_optim_low4*1e9-fmin*1e9)/(((fmax-fmin)*1e9)/length(f)));  
high4=ceil((f_optim_high4*1e9-fmin*1e9)/(((fmax-fmin)*1e9)/length(f)));  
  
low5=floor((f_optim_low5*1e9-fmin*1e9)/(((fmax-fmin)*1e9)/length(f)));  
high5=ceil((f_optim_high5*1e9-fmin*1e9)/(((fmax-fmin)*1e9)/length(f)));
```

```
end
```

```
sintheta=sin(thetaradian);  
costheta=cos(thetaradian);
```

---

```

for m=1:length(theta)

    sinthetal=sintheta(m);
    costhetal=costheta(m);

    %Total reflection and transmission coefficients
    for k =1:length(f);
        lambda_freespace(k)=c/(f(k));
        Gamma=2*(pi/lambda_freespace(k));
        TotalMatrix=1;

    %Characteristic layer impedance
    Er(1)=Ei(1)*(1-(j*tand(1)));
    Z(1)=(costhetal/sqrt(Er(1)-(sinthetal^2)));
    for i=2:N+1
        Er(i)=Ei(i)*(1-(j*tand(i)));
        if polarization==1
            Z(i)=sqrt(Er(i)-(sinthetal^2))/(Er(i)*costhetal);
        elseif polarization==2
            Z(i)=(costhetal/sqrt(Er(i)-(sinthetal^2)));
        end
    end

    %Reflection and transmission for the different layers
    refl(1)=(Z(1)-1)/(Z(1)+1);
    trans(1)=sqrt(1-refl(1)^2);
    for i=2:N+1
        refl(i)=(Z(i)-Z(i-1))/(Z(i)+Z(i-1));
        trans(i)=sqrt(1-refl(i)^2);
    end

    %Wave matrix calculation
    for i =1:(N)
        M=exp(j*Gamma*t(i)*sqrt(Er(i)-(sinthetal^2)));
        Mc=exp(-j*Gamma*t(i)*sqrt(Er(i)-(sinthetal^2)));
        TotalMatrix=TotalMatrix*(1/trans(i))*[M,refl(i)*Mc;refl(i)*M,Mc];
    end

    %Total reflection and transmission coefficients of the structure
    TotalMatrix=1/trans(N+1)*TotalMatrix*[1 refl(N+1); refl(N+1) 1];
    reflection(k)=TotalMatrix(2,1)/TotalMatrix(1,1);
    transmission(k)=1/TotalMatrix(1,1);

end

    Transabs=abs(transmission);
    Reflabs=abs(reflection);
    Transabsdb=mag2db(Transabs);
    Reflabsdb=mag2db(Reflabs);

    %Plot the transmission and reflection coefficients in dB:
    figure(1);

```

---

---

```

plot(f/1e9,Reflabsdb,'k');
grid;
xlabel('Frequency (GHz)');
ylabel('Reflection loss (dB)');
figure(2);
plot(f/1e9,Transabsdb,'k');
grid;
xlabel('Frequency (GHz)');
ylabel('Transmission loss (dB)');

for a=1:length(f);
    E(a)=Reflabsdb(a);
end
end

ehandle=@Wall_Transmission_Optimization_frequency_band;

if z==1
Error=sum(E([low1:high1]));

    elseif z==2
Error=sum(E([low1:high1])+sum(E([low2:high2])));

    elseif z==3
Error=E([low1:high1 low2:high2 low3:high3]);

    elseif z==4
Error=E([low1:high1 low2:high2 low3:high3 low4:high4]);

    elseif z==5
Error=E([low1:high1 low2:high2 low3:high3 low4:high4 low5:high5]);

end

```

---

## Appendix E - Optimization.m

```
ehandle=@Wall_Transmission_Optimization_1_layer;

%Initial values before optimization
Er1_i=3.8;
Er2_i=2.9;
% Er3_i=3.8;
% Er4_i=2.9;
% Er5_i=2.9;
% Er6_i=3.8;
% Er7_i=1.08;
% Er8_i=3.8;
% Er9_i=2.9;
% Er10_i=3.8;

tand1_i=0.001;
tand2_i=0.01;
% tand3_i=0.001;
% tand4_i=0.01;
% tand5_i=0.01;
% tand6_i=0.001;
% tand7_i=0.001;
% tand8_i=0.001;
% tand9_i=0.01;
% tand10_i=0.001;

%Limits (Er 1; tand 1; Er 2; tand 2; Er n; tand n;]
lb=[1;0.0005;1;0.0005];%1;0.001;1;0.005]; %Low limit
ub=[5;0.1;5;0.1];%5;0.1;5;0.05]; %High limit

%options = optimset();
E=lsqnonlin(ehandle,[Er1_i;tand1_i;Er2_i;tand2_i],lb,ub);%;Er3_i;tand3_i;Er4_i;tand4_i], lb, ub);

%Optimized values
Er1_o=E(1);
Er2_o=E(3);
% Er3_o=E(5);
% Er4_o=E(7);
% Er5_o=E(9);
% Er6_o=E(11);
% Er7_o=E(13);
% Er8_o=E(15);
% Er9_o=E(17);
% Er10_o=E(19);

tand1_o=E(2);
tand2_o=E(4);
% tand3_o=E(6);
% tand4_o=E(8);
% tand5_o=E(10);
% tand6_o=E(12);
% tand7_o=E(14);
% tand8_o=E(16);
```

---

```
% tand9_o=E(18);  
% tand10_o=E(20);
```

---

## Appendix F - Optimization\_frequency\_band.m

```
%%%%%%%%%%%%%%%%%%%%%%%%%%%%%%%%%%%%%%%%%%%%%%%%%%%%%%%%%%%%%%%%%%%%%%%%
%Optimization routine for minimum transmission loss over frequency band(s)%
%%%%%%%%%%%%%%%%%%%%%%%%%%%%%%%%%%%%%%%%%%%%%%%%%%%%%%%%%%%%%%%%%%%%%%%%

clear;

ehandle=@Wall_Transmission_Optimization_frequency_band;

%Initial values for optimization
Thickness1_i=0.007;
Thickness2_i=1.0e-2;
Thickness3_i=0.07e-2;
Thickness4_i=20e-3;
Thickness5_i=20e-3;

%Lower and upper optimization bounds for the individual layers
lb1=0.006;
lb2=0.8e-2;
lb3=0.06e-2;
lb4=18e-3;
lb5=4e-3;

ub1=0.009;
ub2=1.2e-2;
ub3=0.09e-2;
ub4=22e-3;
ub5=6e-3;

%Maximum number of optimization iterations
Iter=50;

%%%%%%%%%%%%%%%%%%%%%%%%%%%%%%%%%%%%%%%%%%%%%%%%%%%%%%%%%%%%%%%%%%%%%%%%
%      Optimization for n frequency bands      %
%      Uncomment the actual number of layers  %
%%%%%%%%%%%%%%%%%%%%%%%%%%%%%%%%%%%%%%%%%%%%%%%%%%%%%%%%%%%%%%%%%%%%%%%%

% %1 layer
%
options = optimset('MaxIter',Iter);
E=fminsearchbnd(ehandle,[Thickness1_i],lb1,ub1,options);

%Optimized value 1 layer
Thickness1_o=E(1);

% %2 layers
%
% lb=[lb1,lb2];
% ub=[ub1,ub2];
%
% options = optimset('MaxIter',Iter);
% E=fminsearchbnd(ehandle,[Thickness1_i,Thickness2_i],lb,ub,options);
%
% %Optimized value 2 layers
```

---

```

% Thickness1_o=E(1);
% Thickness2_o=E(2);
%
% %3 layers
%
% lb=[lb1,lb2,lb3];
% ub=[ub1,ub2,ub3];
%
% options = optimset('MaxIter',Iter);
% E=fminsearchbnd(ehandle,[Thickness1_i,Thickness2_i,Thickness3_i],lb,ub,options);
%
% %Optimized value 1 layers
% Thickness1_o=E(1);
% Thickness2_o=E(2);
% Thickness3_o=E(3);

% %4 layers

% lb=[lb1,lb2,lb3,lb4];
% ub=[ub1,ub2,ub3,ub4];
%
% options = optimset('MaxIter',Iter);
% E=fminsearchbnd(ehandle,[Thickness1_i,Thickness2_i,Thickness3_i,Thickness4_i],lb,ub,options);
%
% %Optimized value 4 layers
% Thickness1_o=E(1);
% Thickness2_o=E(2);
% Thickness3_o=E(3);
% Thickness4_o=E(4);

% %5 layers

% lb=[lb1,lb2,lb3,lb4,lb5];
% ub=[ub1,ub2,ub3,ub4,ub5];

% options = optimset('MaxIter',Iter);
% E=fminsearchbnd(ehandle,[Thickness1_i,Thickness2_i,Thickness3_i,Thickness4_i,Thickness5_i],lb,ub,options);
%
% %Optimized value 5 layers
% Thickness1_o=E(1);
% Thickness2_o=E(2);
% Thickness3_o=E(3);
% Thickness4_o=E(4);
% Thickness5_o=E(5);

```



---

## Appendix G - fminsearchbnd.m

```
function [x,fval,exitflag,output] = fminsearchbnd(fun,x0,LB,UB,options,varargin)
% FMINSEARCHBND: FMINSEARCH, but with bound constraints by transformation
% usage: x=FMINSEARCHBND(fun,x0)
% usage: x=FMINSEARCHBND(fun,x0,LB)
% usage: x=FMINSEARCHBND(fun,x0,LB,UB)
% usage: x=FMINSEARCHBND(fun,x0,LB,UB,options)
% usage: x=FMINSEARCHBND(fun,x0,LB,UB,options,p1,p2,...)
% usage: [x,fval,exitflag,output]=FMINSEARCHBND(fun,x0,...)
%
% arguments:
% fun, x0, options - see the help for FMINSEARCH
%
% LB - lower bound vector or array, must be the same size as x0
%
% If no lower bounds exist for one of the variables, then
% supply -inf for that variable.
%
% If no lower bounds at all, then LB may be left empty.
%
% Variables may be fixed in value by setting the corresponding
% lower and upper bounds to exactly the same value.
%
% UB - upper bound vector or array, must be the same size as x0
%
% If no upper bounds exist for one of the variables, then
% supply +inf for that variable.
%
% If no upper bounds at all, then UB may be left empty.
%
% Variables may be fixed in value by setting the corresponding
% lower and upper bounds to exactly the same value.
%
% Notes:
%
% If options is supplied, then TolX will apply to the transformed
% variables. All other FMINSEARCH parameters should be unaffected.
%
% Variables which are constrained by both a lower and an upper
% bound will use a sin transformation. Those constrained by
% only a lower or an upper bound will use a quadratic
% transformation, and unconstrained variables will be left alone.
%
% Variables may be fixed by setting their respective bounds equal.
% In this case, the problem will be reduced in size for FMINSEARCH.
%
% The bounds are inclusive inequalities, which admit the
% boundary values themselves, but will not permit ANY function
% evaluations outside the bounds. These constraints are strictly
% followed.
%
% If your problem has an EXCLUSIVE (strict) constraint which will
% not admit evaluation at the bound itself, then you must provide
% a slightly offset bound. An example of this is a function which
```

---

```

% contains the log of one of its parameters. If you constrain the
% variable to have a lower bound of zero, then FMINSEARCHBND may
% try to evaluate the function exactly at zero.
%
%
% Example usage:
% rosen = @(x) (1-x(1)).^2 + 105*(x(2)-x(1).^2).^2;
%
% fminsearch(rosen,[3 3])      % unconstrained
% ans =
%     1.0000     1.0000
%
% fminsearchbnd(rosen,[3 3],[2 2],[]) % constrained
% ans =
%     2.0000     4.0000
%
% See test_main.m for other examples of use.
%
%
% See also: fminsearch, fminspleas
%
%
% Author: John D'Errico
% E-mail: woodchips@rochester.rr.com
% Release: 4
% Release date: 7/23/06

% size checks
xsize = size(x0);
x0 = x0(:);
n=length(x0);

if (nargin<3) || isempty(LB)
    LB = repmat(-inf,n,1);
else
    LB = LB(:);
end
if (nargin<4) || isempty(UB)
    UB = repmat(inf,n,1);
else
    UB = UB(:);
end

if (n~=length(LB)) || (n~=length(UB))
    error 'x0 is incompatible in size with either LB or UB.'
end

% set default options if necessary
if (nargin<5) || isempty(options)
    options = optimset('fminsearch');
end

% stuff into a struct to pass around
params.args = varargin;
params.LB = LB;
params.UB = UB;
params.fun = fun;

```

---

```

params.n = n;
% note that the number of parameters may actually vary if
% a user has chosen to fix one or more parameters
params.xsize = xsize;
params.OutputFcn = [];

% 0 --> unconstrained variable
% 1 --> lower bound only
% 2 --> upper bound only
% 3 --> dual finite bounds
% 4 --> fixed variable
params.BoundClass = zeros(n,1);
for i=1:n
    k = isfinite(LB(i)) + 2*isfinite(UB(i));
    params.BoundClass(i) = k;
    if (k==3) && (LB(i)==UB(i))
        params.BoundClass(i) = 4;
    end
end

% transform starting values into their unconstrained
% surrogates. Check for infeasible starting guesses.
x0u = x0;
k=1;
for i = 1:n
    switch params.BoundClass(i)
        case 1
            % lower bound only
            if x0(i) <= LB(i)
                % infeasible starting value. Use bound.
                x0u(k) = 0;
            else
                x0u(k) = sqrt(x0(i) - LB(i));
            end

            % increment k
            k=k+1;
        case 2
            % upper bound only
            if x0(i) >= UB(i)
                % infeasible starting value. use bound.
                x0u(k) = 0;
            else
                x0u(k) = sqrt(UB(i) - x0(i));
            end

            % increment k
            k=k+1;
        case 3
            % lower and upper bounds
            if x0(i) <= LB(i)
                % infeasible starting value
                x0u(k) = -pi/2;
            elseif x0(i) >= UB(i)
                % infeasible starting value
                x0u(k) = pi/2;
            else

```

---

```

    x0u(k) = 2*(x0(i) - LB(i))/(UB(i)-LB(i)) - 1;
    % shift by 2*pi to avoid problems at zero in fminsearch
    % otherwise, the initial simplex is vanishingly small
    x0u(k) = 2*pi+asin(max(-1,min(1,x0u(k))));
end

    % increment k
    k=k+1;
case 0
    % unconstrained variable. x0u(i) is set.
    x0u(k) = x0(i);

    % increment k
    k=k+1;
case 4
    % fixed variable. drop it before fminsearch sees it.
    % k is not incremented for this variable.
end

end

end
% if any of the unknowns were fixed, then we need to shorten
% x0u now.
if k<=n
    x0u(k:n) = [];
end

% were all the variables fixed?
if isempty(x0u)
    % All variables were fixed. quit immediately, setting the
    % appropriate parameters, then return.

    % undo the variable transformations into the original space
    x = xtransform(x0u,params);

    % final reshape
    x = reshape(x,xsize);

    % stuff fval with the final value
    fval = feval(params.fun,x,params.args{:});

    % fminsearchbnd was not called
    exitflag = 0;

    output.iterations = 0;
    output.funcCount = 1;
    output.algorithm = 'fminsearch';
    output.message = 'All variables were held fixed by the applied bounds';

    % return with no call at all to fminsearch
    return
end

% Check for an outputfcn. If there is any, then substitute my
% own wrapper function.
if ~isempty(options.OutputFcn)
    params.OutputFcn = options.OutputFcn;
    options.OutputFcn = @outfun_wrapper;

```

---

---

**end**

```
% now we can call fminsearch, but with our own  
% intra-objective function.  
[xu,fval,exitflag,output] = fminsearch(@intrafun,x0u,options,params);  
  
% undo the variable transformations into the original space  
x = xtransform(xu,params);  
  
% final reshape to make sure the result has the proper shape  
x = reshape(x,xsize);  
  
% Use a nested function as the OutputFcn wrapper  
function stop = outfun_wrapper(x,varargin);  
    % we need to transform x first  
    xtrans = xtransform(x,params);  
  
    % then call the user supplied OutputFcn  
    stop = params.OutputFcn(xtrans,varargin{1:(end-1)});
```

**end**

**end** *% mainline end*

```
% =====  
% ===== begin subfunctions =====  
% =====  
function fval = intrafun(x,params)  
% transform variables, then call original function  
  
% transform  
xtrans = xtransform(x,params);  
  
% and call fun  
fval = feval(params.fun,reshape(xtrans,params.xsize),params.args{:});
```

**end** *% sub function intrafun end*

```
% =====  
function xtrans = xtransform(x,params)  
% converts unconstrained variables into their original domains  
  
xtrans = zeros(params.xsize);  
% k allows some variables to be fixed, thus dropped from the  
% optimization.  
k=1;  
for i = 1:params.n  
    switch params.BoundClass(i)  
        case 1  
            % lower bound only  
            xtrans(i) = params.LB(i) + x(k).^2;  
  
            k=k+1;  
        case 2  
            % upper bound only  
            xtrans(i) = params.UB(i) - x(k).^2;
```

---

```
    k=k+1;
case 3
    % lower and upper bounds
    xtrans(i) = (sin(x(k))+1)/2;
    xtrans(i) = xtrans(i)*(params.UB(i) - params.LB(i)) + params.LB(i);
    % just in case of any floating point problems
    xtrans(i) = max(params.LB(i),min(params.UB(i),xtrans(i)));

    k=k+1;
case 4
    % fixed variable, bounds are equal, set it at either bound
    xtrans(i) = params.LB(i);
case 0
    % unconstrained variable.
    xtrans(i) = x(k);

    k=k+1;
end
end

end % sub function xtransform end
```